

TABLE 1
IRON LINES AND EQUIVALENT WIDTH MEASUREMENTS

Ion	$\lambda(\text{\AA})$	χ (eV)	gf	W (m\AA)
Fe I	6024.058	4.548	8.710e-01	109
	6027.051	4.076	8.128e-02	69
	6056.005	4.733	3.981e-01	81
	6079.009	4.652	1.072e-01	50
	6096.665	3.984	1.660e-02	39
	6151.618	2.176	5.129e-04	47
	6157.728	4.076	7.762e-02	72
	6165.360	4.142	3.388e-02	46
	6173.336	2.223	1.318e-03	69
	6187.990	3.943	2.692e-02	47
	6380.743	4.186	4.786e-02	54
	6411.649	3.653	2.188e-01	122
	6421.351	2.279	9.772e-03	124
	6469.193	4.835	2.399e-01	68
	6593.871	2.437	3.802e-03	87
	6597.561	4.795	1.202e-01	47
	6609.110	2.559	2.042e-03	65
	6733.151	4.637	3.715e-02	27
	6820.372	4.638	6.761e-02	40
	6858.150	4.607	1.175e-01	55
Fe II	6084.099	3.199	1.585e-04	37
	6149.246	3.889	1.905e-03	63
	6416.921	3.891	2.089e-03	63
	6432.682	2.891	2.630e-04	63

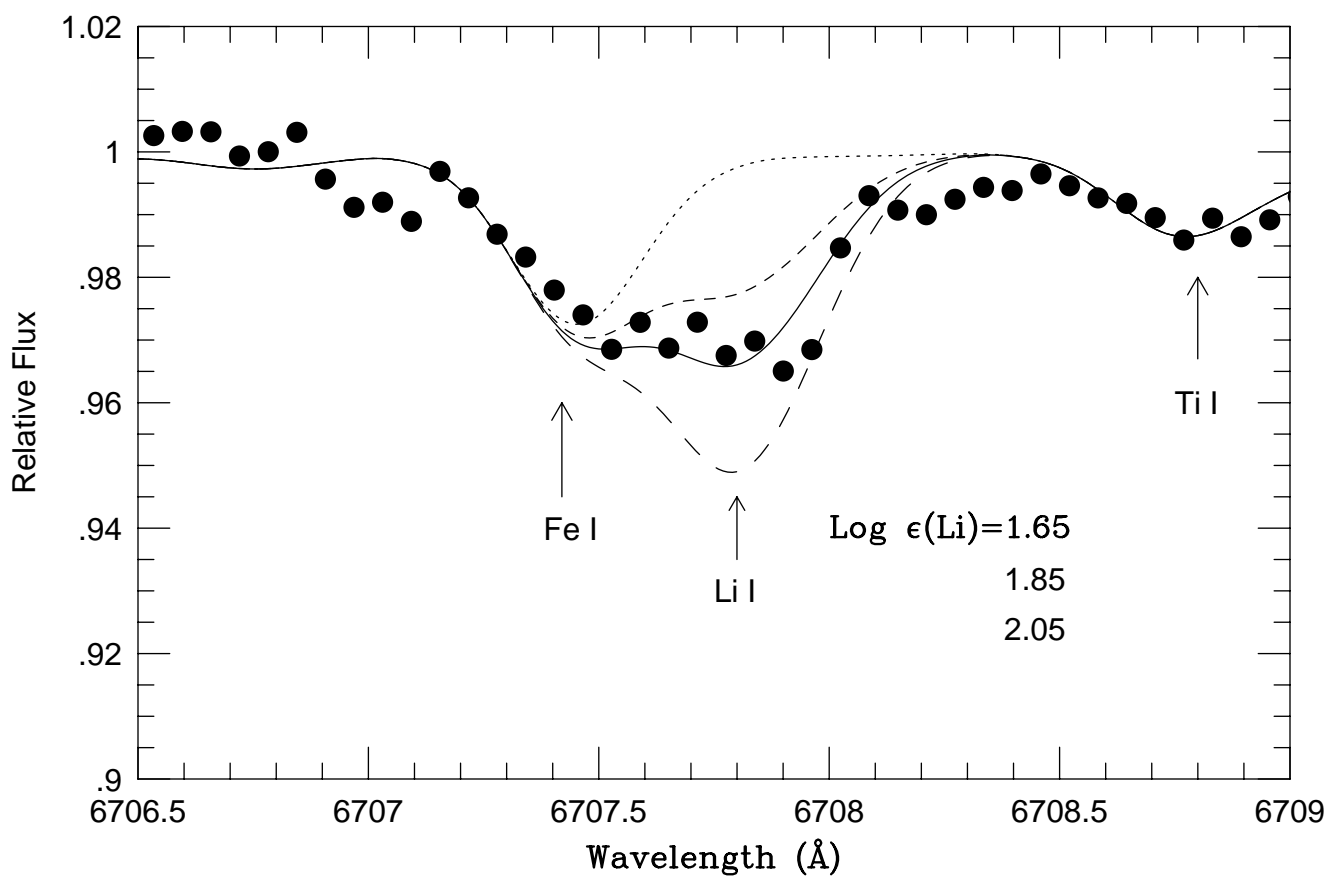
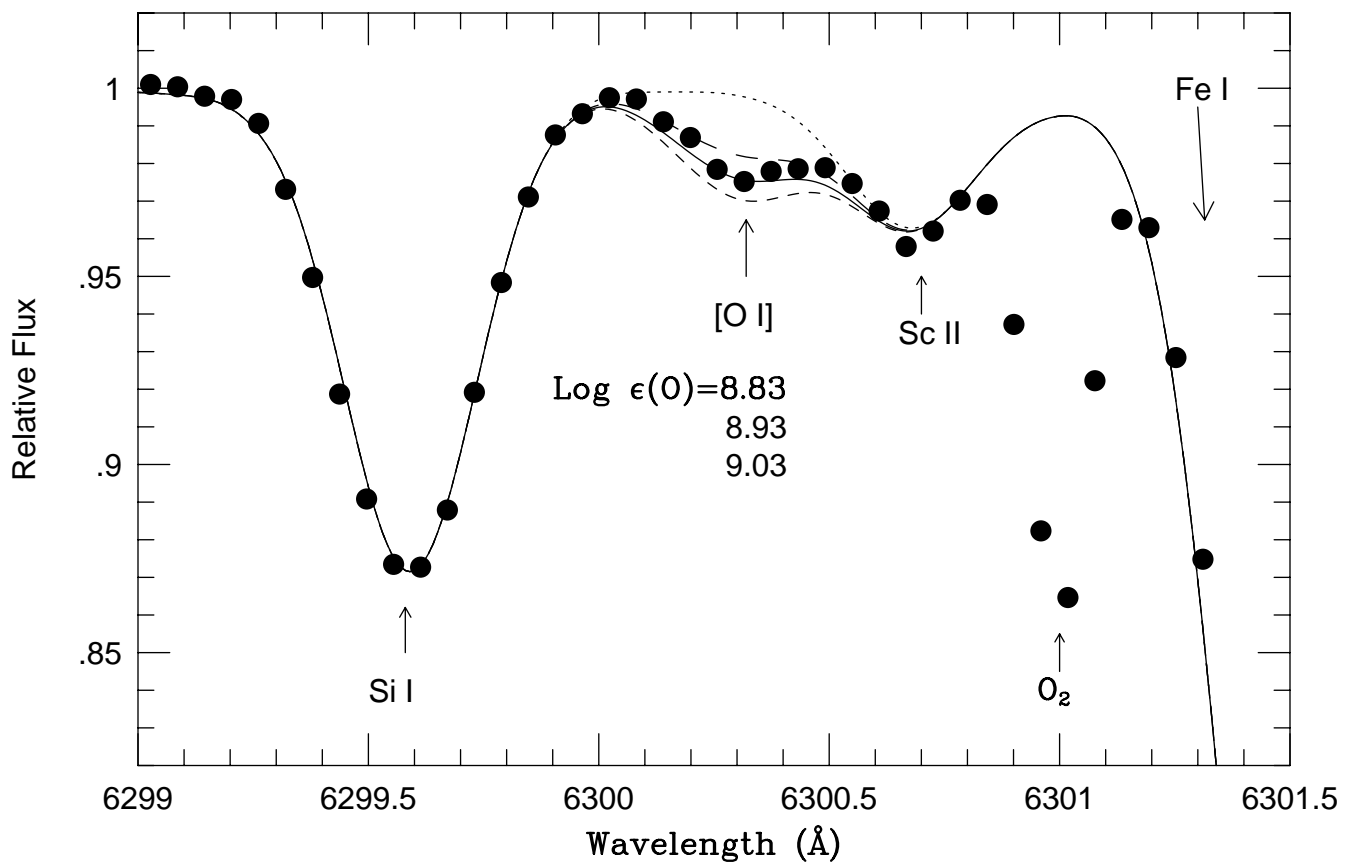


TABLE 2
PHYSICAL PROPERTIES FOR HD19994

Hipparcos Parallax	44.69 ± 0.75 mas
Distance	22.4 ± 0.4 pc
V-Magnitude (V)	5.06
Absolute V-Magnitude (M_v)	3.30 ± 0.04
Bolometric Correction	0.10 mag
Luminosity (in L_\odot)	4.46 ± 0.16
Effective Temperature (K)	6030 ± 20
Log g (in cm s^{-2})	3.95 ± 0.05
Spectroscopic Mass (in M_\odot)	1.24 ± 0.14
Spectral Type	F8 V

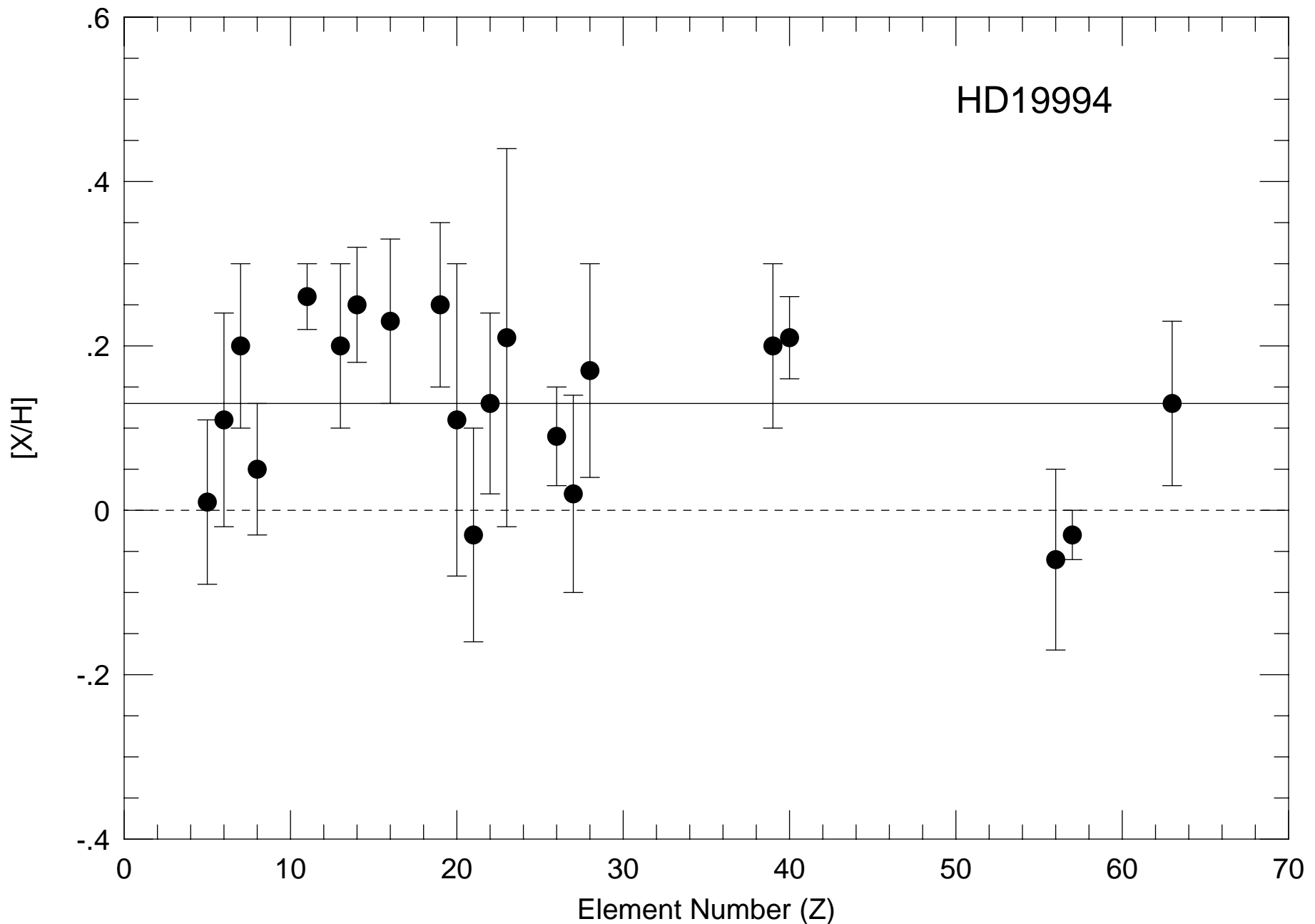


TABLE 3
EQUIVALENT WIDTH MEASUREMENTS FOR HD19994

Ion	λ (Å)	χ (eV)	gf	W (mÅ)
Li I	6707.811	0.000	1.483e+00	ss
C I	6587.610	8.537	6.310e-02	40
	7111.472	8.640	7.413e-02	16
	7113.178	8.647	1.549e-01	47
	7115.172	8.643	1.950e-01	42
	7116.991	8.647	1.148e-01	56
N I	7468.312	10.336	9.550e-01	13
O I	7771.944	9.146	2.109e+00	124
	7774.166	9.146	1.493e+00	106
	7775.388	9.146	8.995e-01	91
	6156.760	10.741	3.331e-01	ss
	6158.180	10.741	4.682e-01	ss
[O I]	6300.311	0.000	1.698e-10	ss
Na I	6154.200	2.102	2.951e-02	47
	6160.800	2.104	5.888e-02	68
Al I	6696.023	3.143	4.786e-02	47
	6698.673	3.143	2.399e-02	23
Si I	6125.021	5.614	2.884e-02	43
	6145.016	5.616	3.802e-02	54
	6721.840	5.860	7.244e-02	62
S I	6052.674	7.870	2.287e-01	28
K I	7698.974	0.000	6.761e-01	158
Ca I	6161.300	2.523	9.333e-02	63
	6166.440	2.521	7.244e-02	71
	6439.080	2.526	2.950e+00	175
	6455.600	2.523	4.571e-02	57
	6471.660	2.526	2.061e-01	113
	6493.780	2.521	7.760e-01	126
	6499.650	2.523	1.510e-01	89
	6508.840	2.526	7.762e-03	6
Sc II	6245.620	1.507	9.550e-02	53
	6604.600	1.357	4.900e-02	50
Ti I	6091.180	2.267	3.802e-01	14
	6126.220	1.067	3.802e-02	18
	6258.100	1.443	4.467e-01	49
	6261.100	1.430	3.311e-01	46
	6554.220	1.443	6.030e-02	10
	6556.060	1.460	6.030e-02	25
	6599.110	0.900	8.222e-03	7
Ti II	6606.970	2.061	1.622e-03	18
V I	6357.292	1.849	1.230e-01	1
	6531.415	1.218	1.445e-01	23
	6785.008	1.051	1.413e-02	6
Co I	6454.990	3.632	5.623e-01	10
	6814.942	1.956	1.995e-02	18
Ni I	6327.600	1.676	7.709e-04	38
	6532.890	1.935	4.074e-04	27
	6586.330	1.951	1.549e-03	40
	6643.640	1.676	5.012e-03	94
	6767.770	1.826	6.761e-03	83

TABLE 3—*Continued*

Ion	λ (Å)	χ (eV)	gf	W (mÅ)
Ni I	6772.360	3.658	1.047e-01	55
Y I	6435.004	0.066	1.514e-01	2
Y II	6795.414	1.738	7.244e-02	10
Zr I	6127.460	0.154	8.710e-02	1
	6134.570	0.000	5.248e-02	3
	6140.460	0.519	3.890e-02	1
	6143.180	0.071	7.943e-02	4
Ba II	6141.730	0.704	8.375e-01	132
	6496.900	0.604	4.170e-01	117
La II	6390.477	0.321	3.548e-02	5
	6774.268	0.126	1.622e-02	4
Eu II	6645.110	1.370	1.580e+00	ss

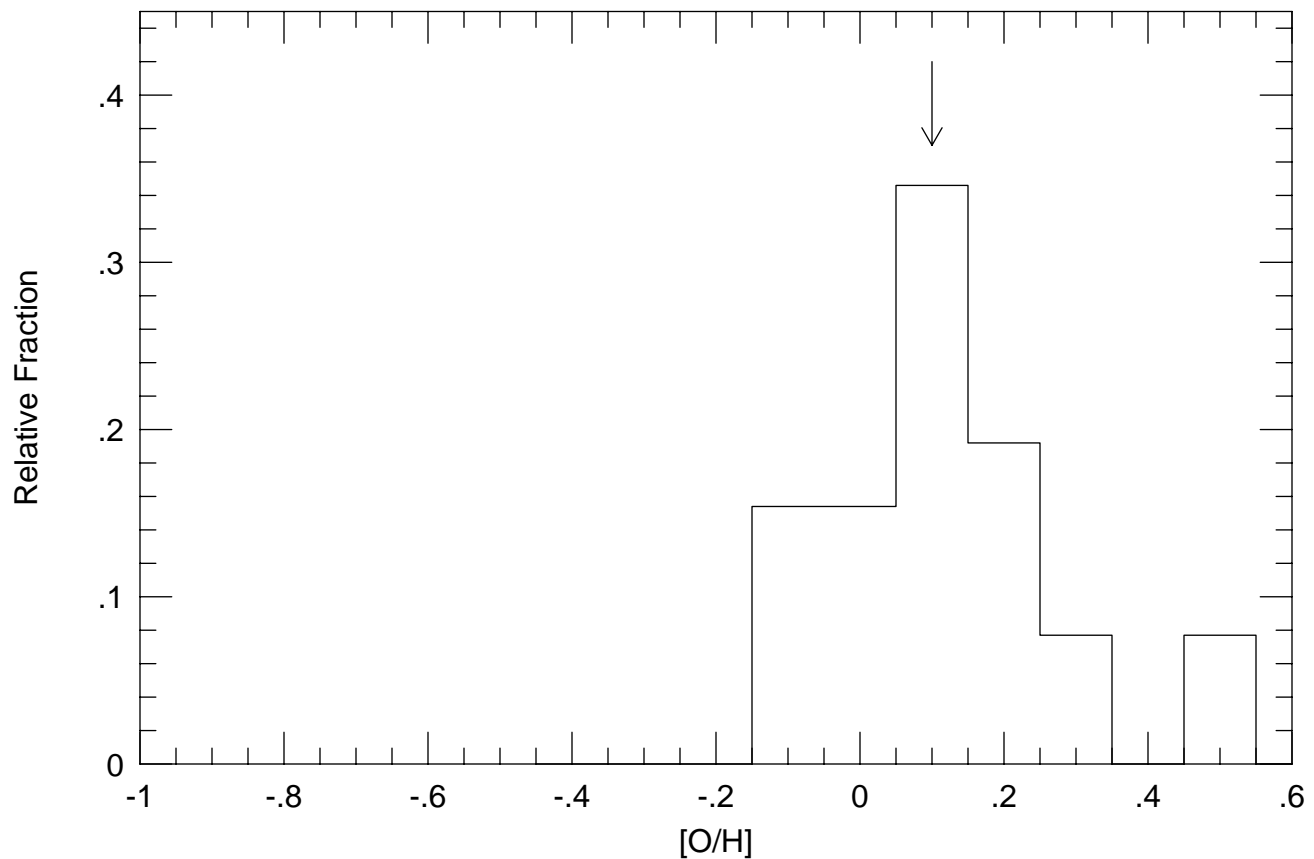
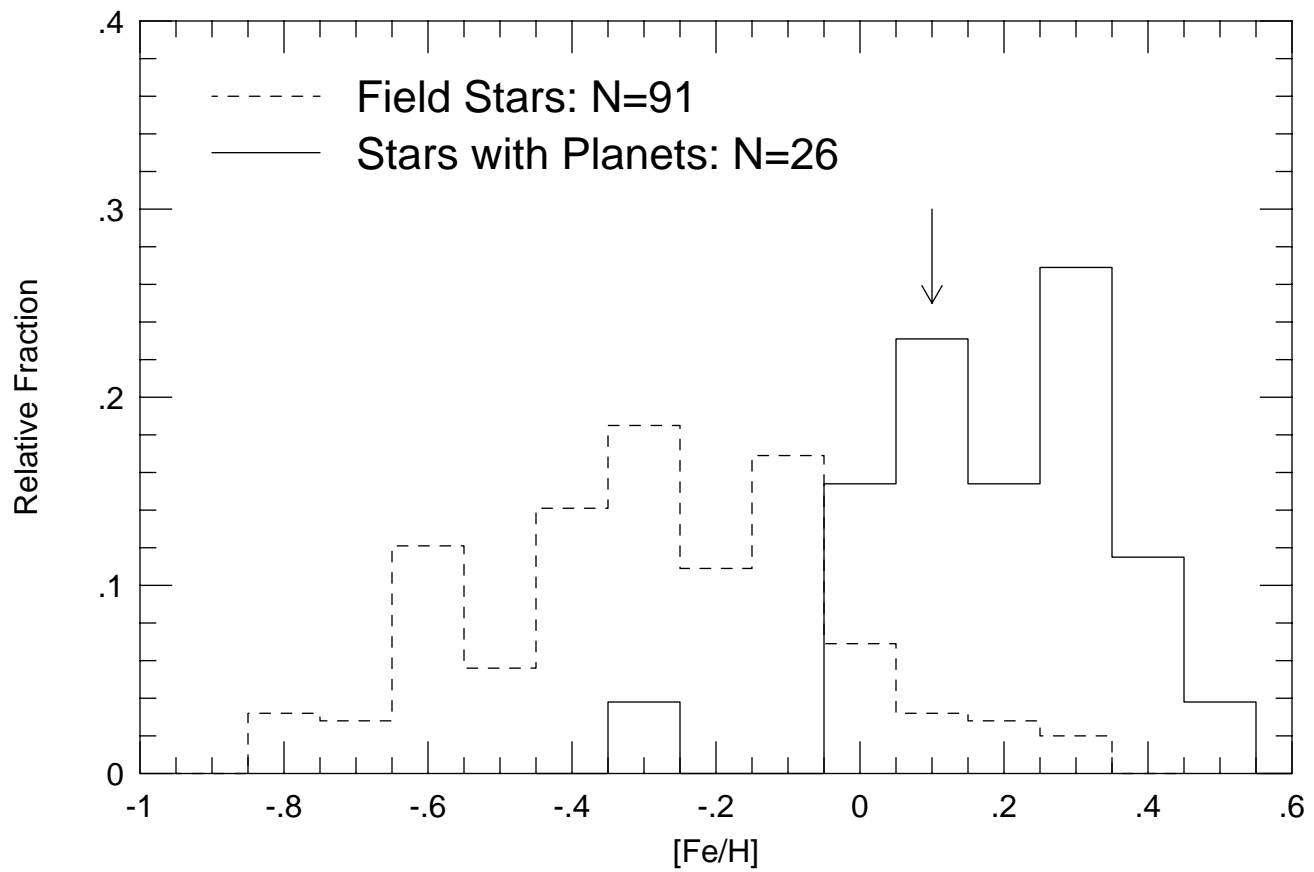
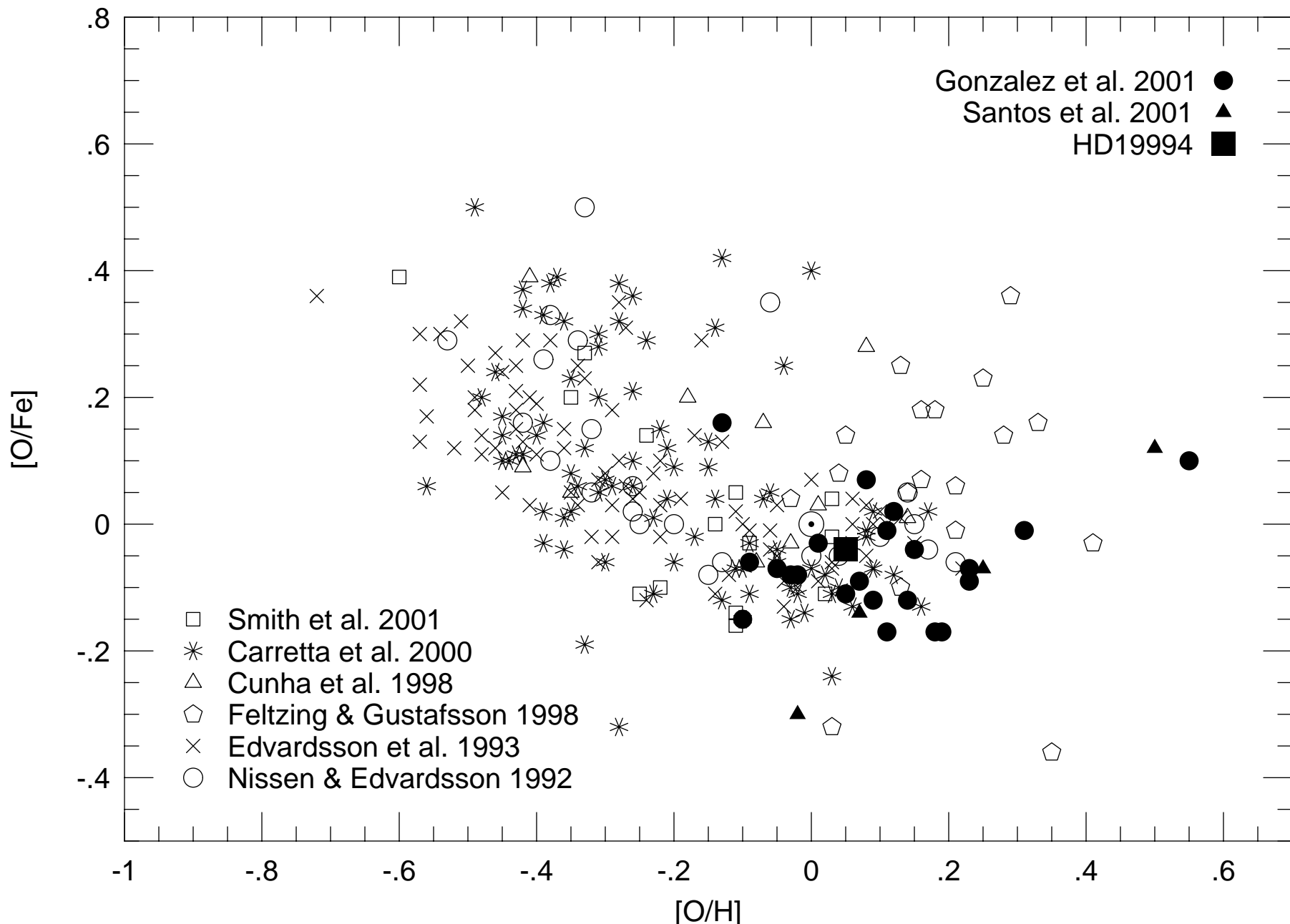
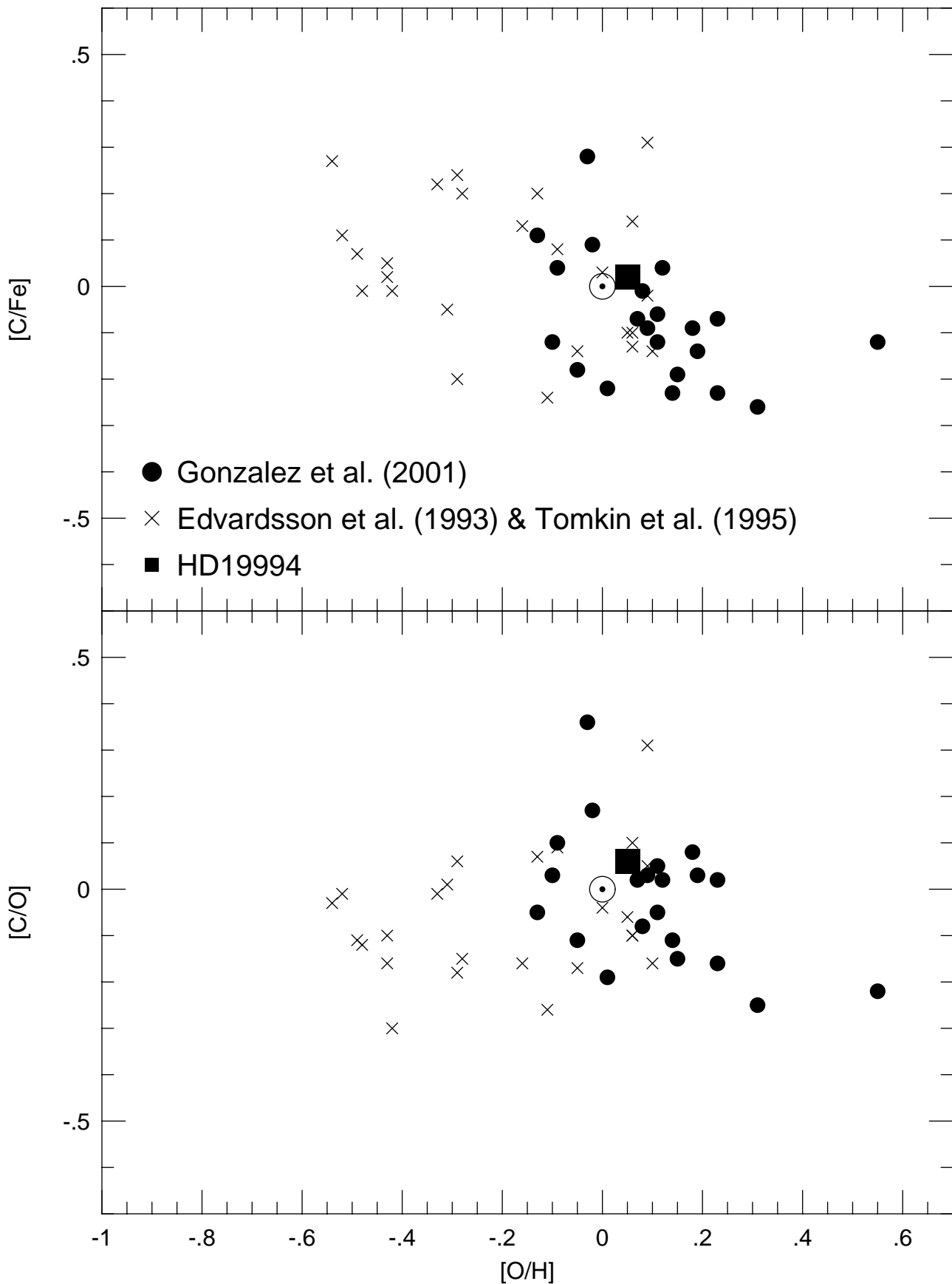
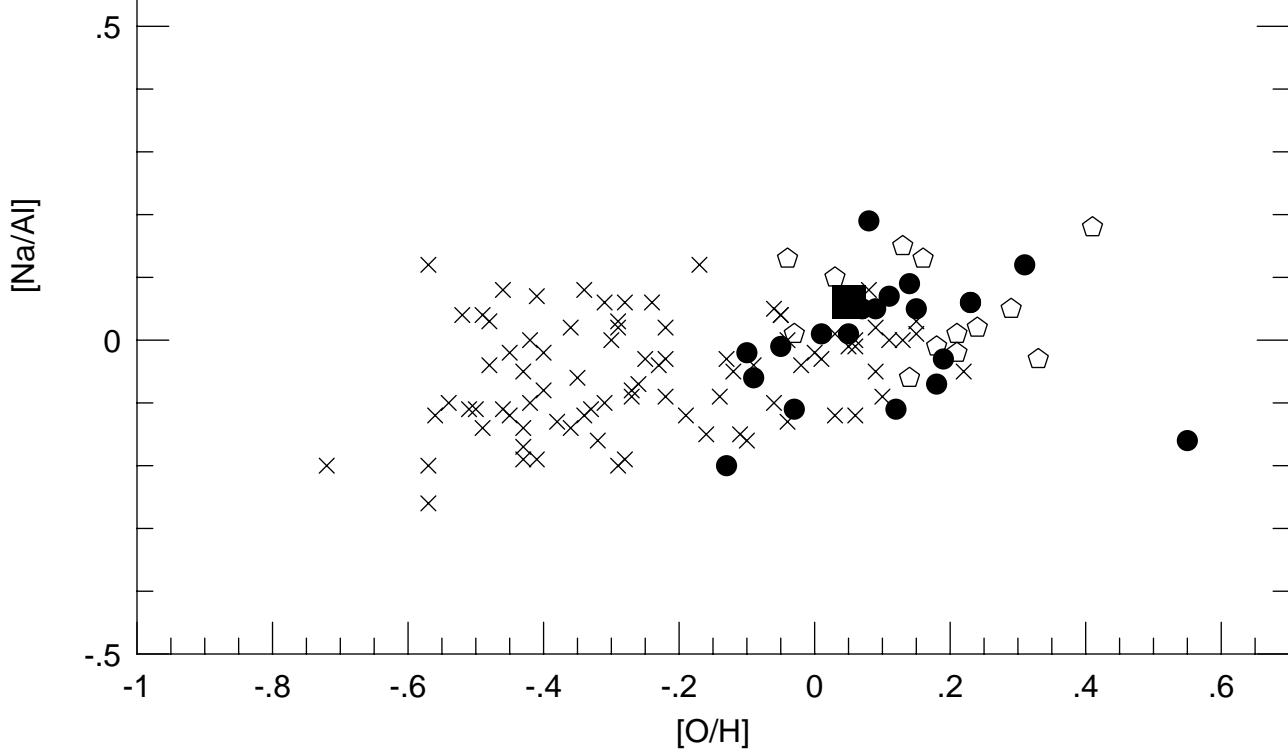
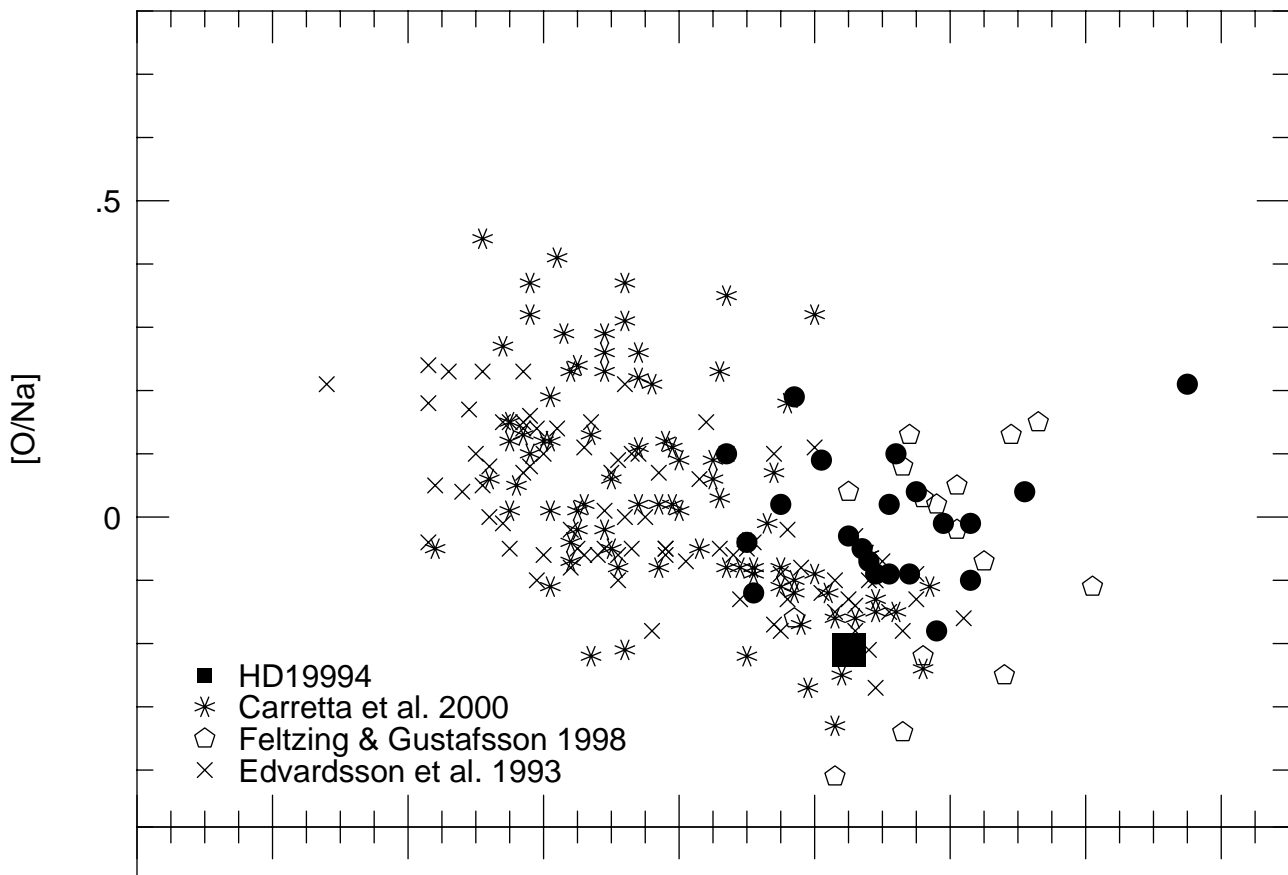


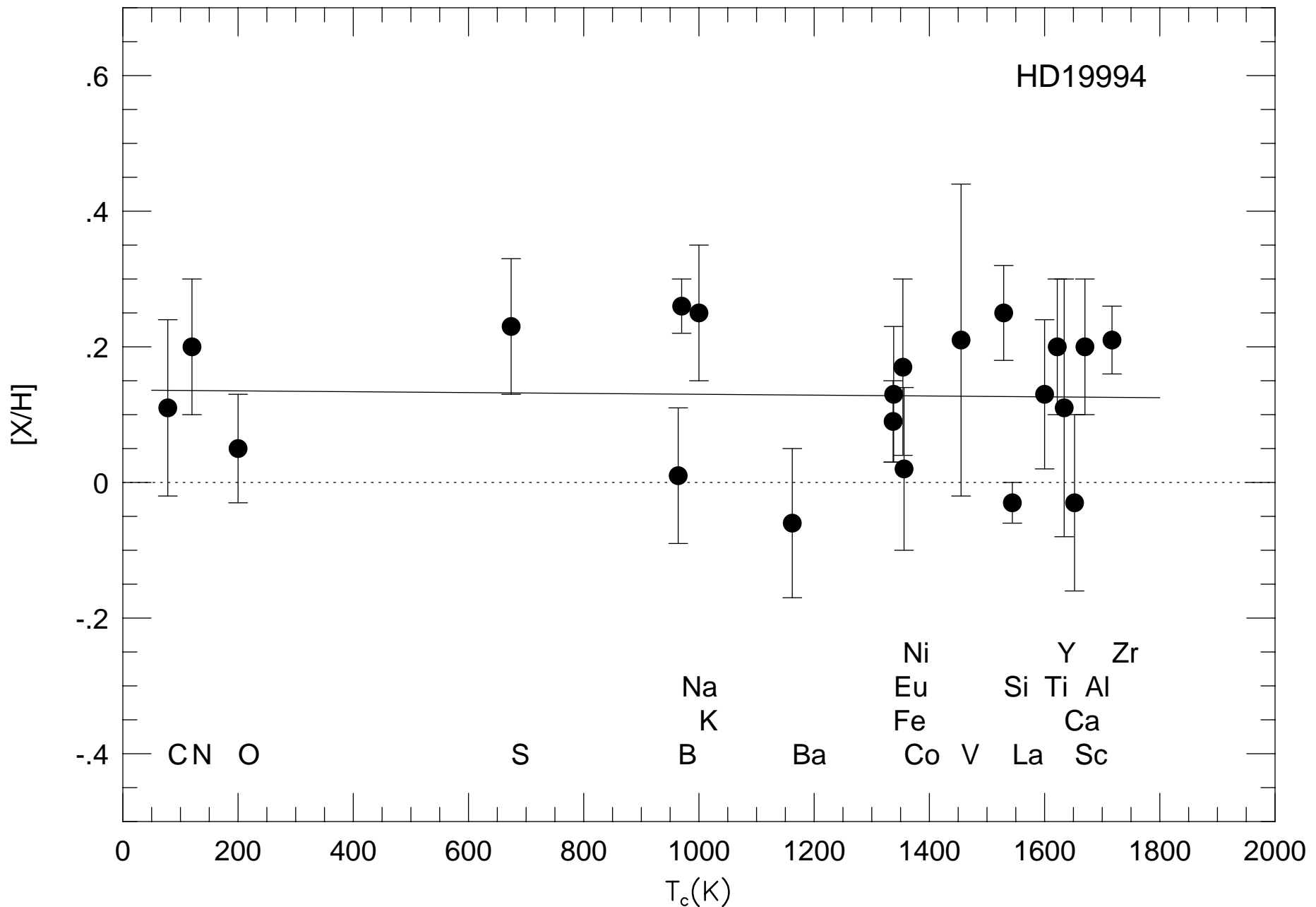
TABLE 4
ABUNDANCES FOR THE SUN AND HD19994

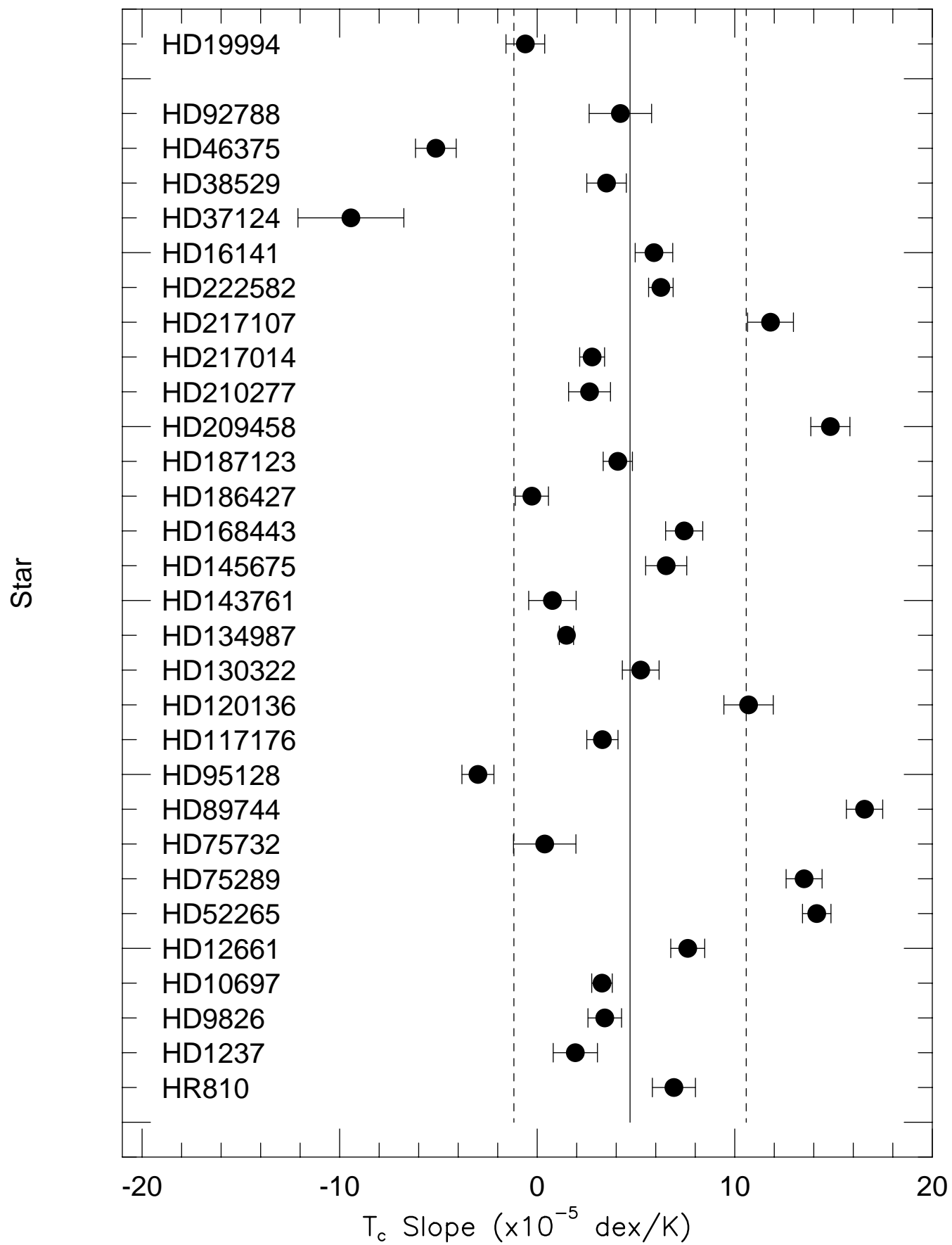
Species	Log $\epsilon(x)_{\odot}$	Log $\epsilon(x)_{HD19994}$	[X/H]
Fe I	7.45 \pm 0.03	7.55 \pm 0.05	+0.10 \pm 0.06
Fe II	7.48 \pm 0.03	7.56 \pm 0.04	+0.08 \pm 0.05
Li I	1.15	1.81	+0.66
B I	2.70	2.71	+0.01
C I	8.54 \pm 0.01	8.65 \pm 0.13	+0.11 \pm 0.13
N I	7.90	8.10	+0.20
O I	8.85 \pm 0.05	8.90 \pm 0.06	+0.05 \pm 0.08
Na I	6.20 \pm 0.03	6.46 \pm 0.02	+0.26 \pm 0.04
Al I	6.20 \pm 0.03	6.40 \pm 0.10	+0.20 \pm 0.10
Si I	7.49 \pm 0.06	7.74 \pm 0.03	+0.25 \pm 0.07
S I	7.27	7.50	+0.23
K I	5.17	5.42	+0.25
Ca I	6.19 \pm 0.08	6.30 \pm 0.17	+0.11 \pm 0.19
Sc II	3.20 \pm 0.11	3.17 \pm 0.06	-0.03 \pm 0.13
Ti I	4.95 \pm 0.05	5.07 \pm 0.10	+0.12 \pm 0.11
Ti II	4.92	5.07	+0.15
V I	4.19 \pm 0.15	4.40 \pm 0.20	+0.21 \pm 0.23
Co I	4.83 \pm 0.04	4.85 \pm 0.11	+0.02 \pm 0.12
Ni I	6.25 \pm 0.03	6.42 \pm 0.13	+0.17 \pm 0.13
Y I	2.26	2.57	+0.31
Y II	2.24	2.33	+0.09
Zr I	2.89 \pm 0.03	3.10 \pm 0.04	+0.21 \pm 0.05
Ba II	2.26 \pm 0.10	2.20 \pm 0.04	-0.06 \pm 0.11
La II	1.22 \pm 0.01	1.19 \pm 0.02	-0.03 \pm 0.03
Eu II	0.55	0.68	+0.13

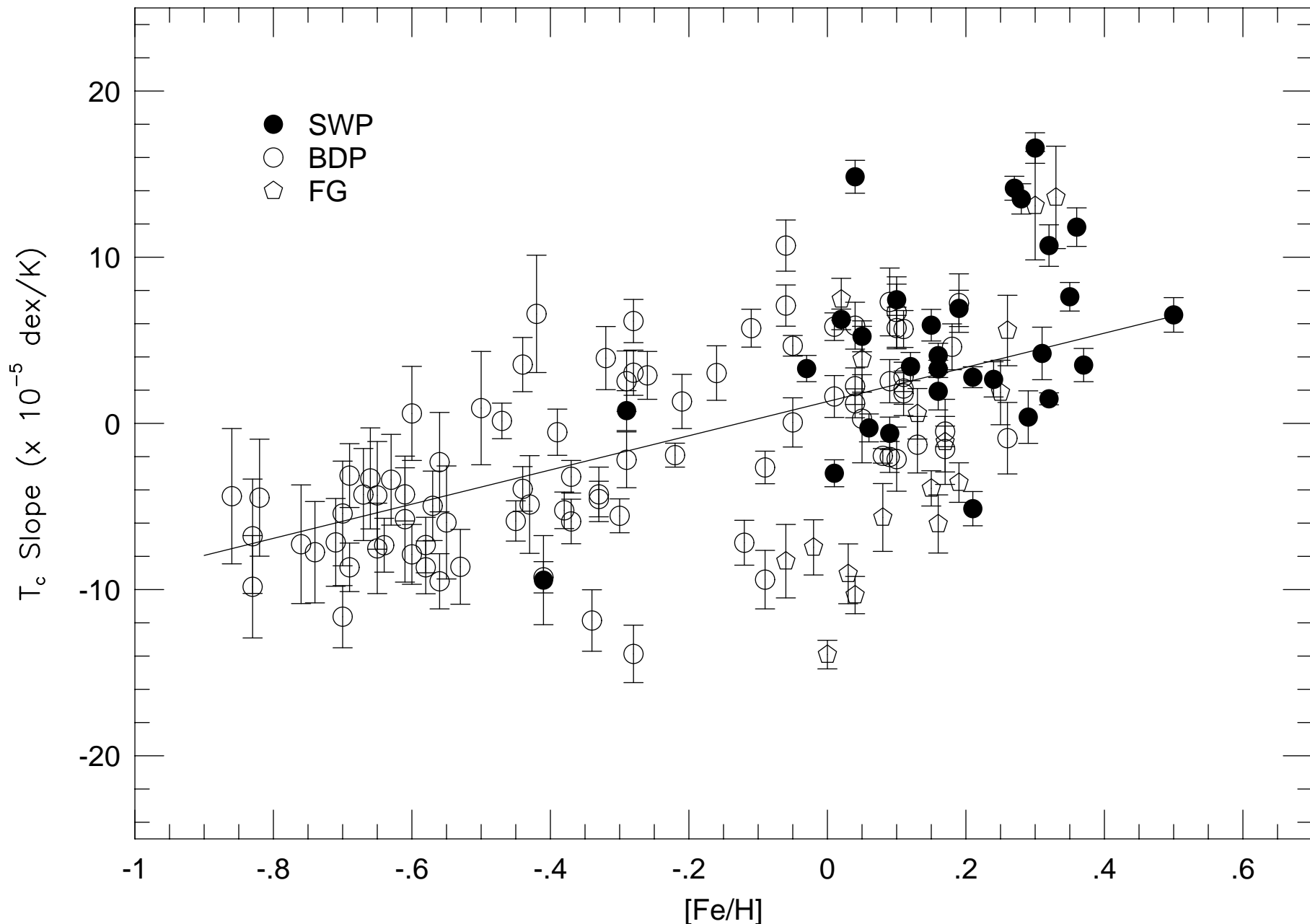


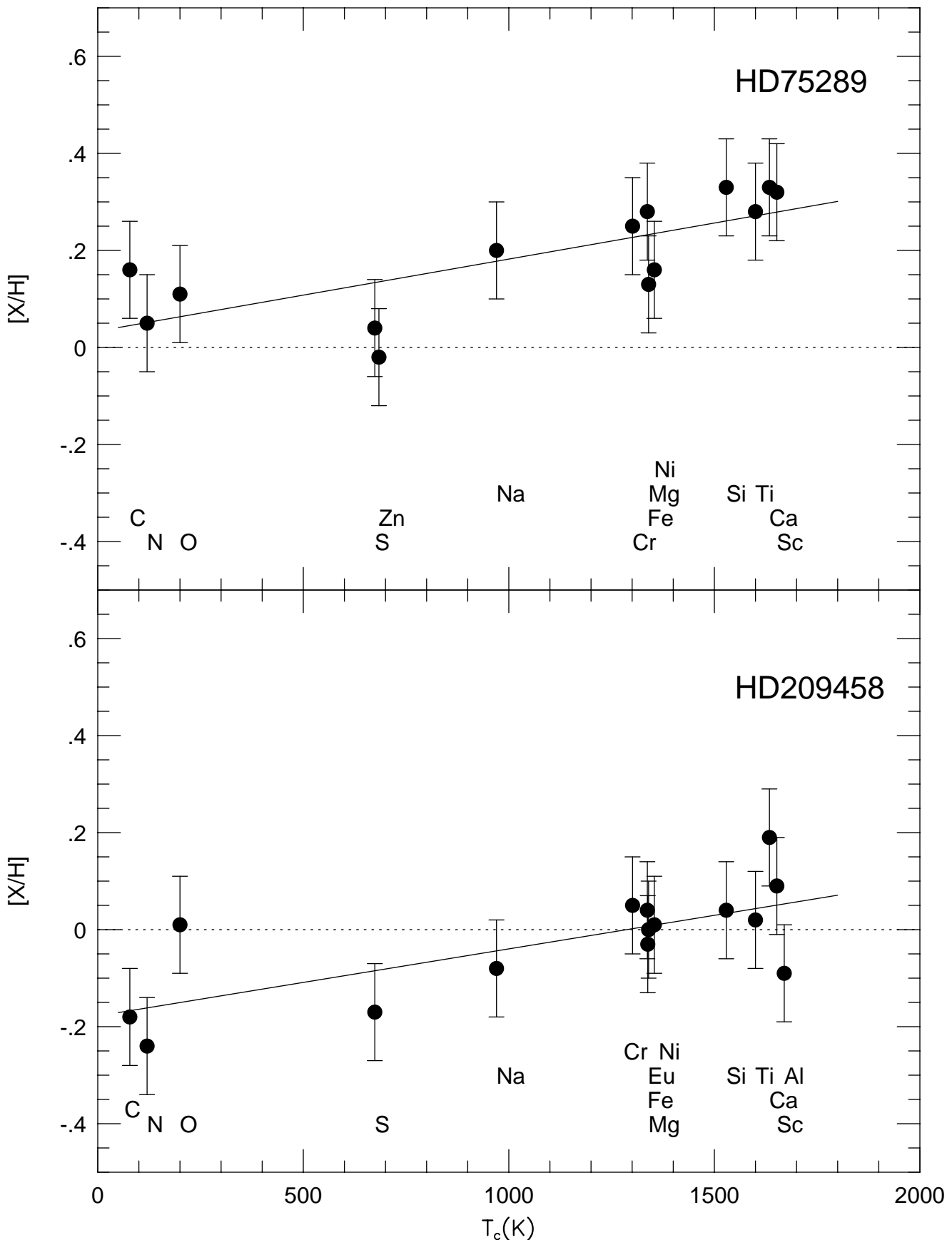


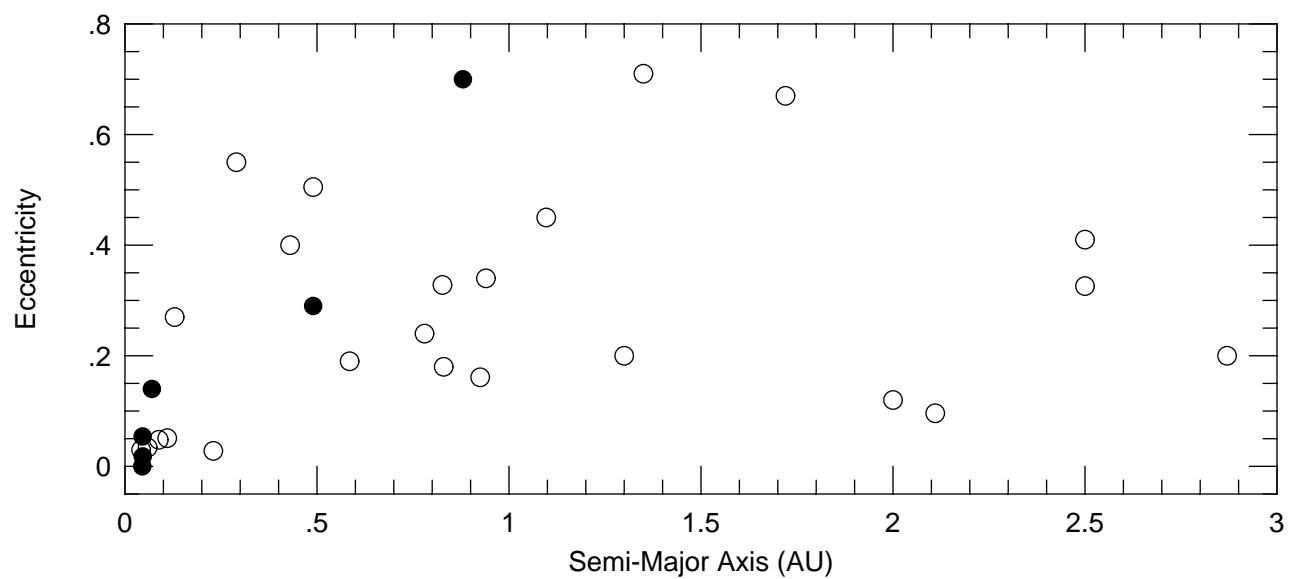
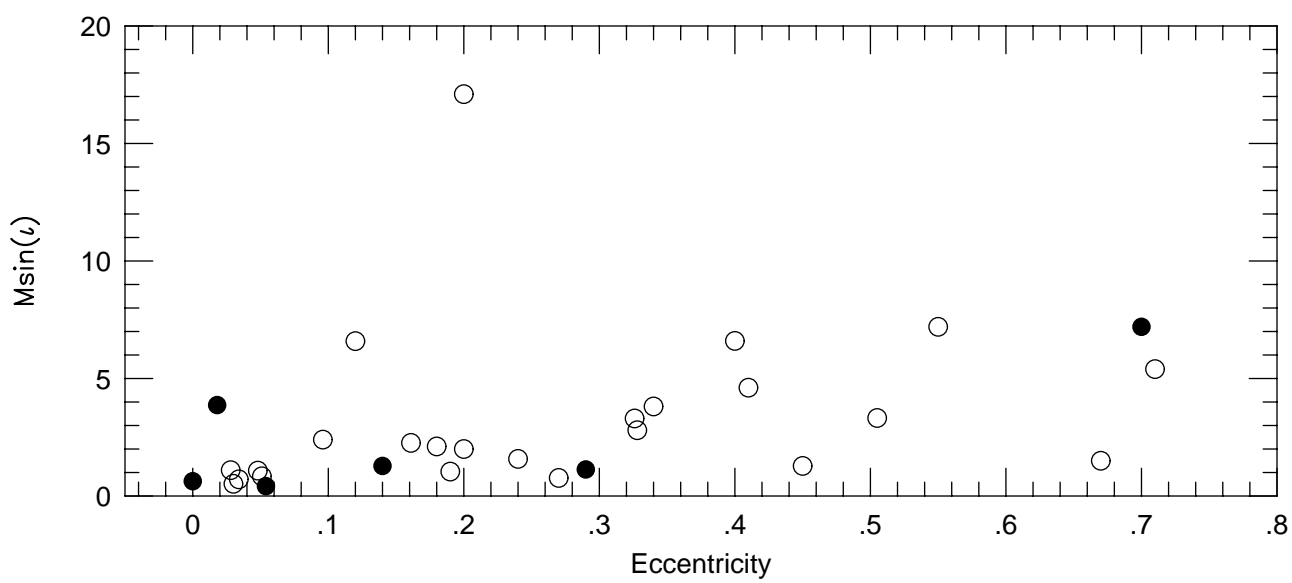
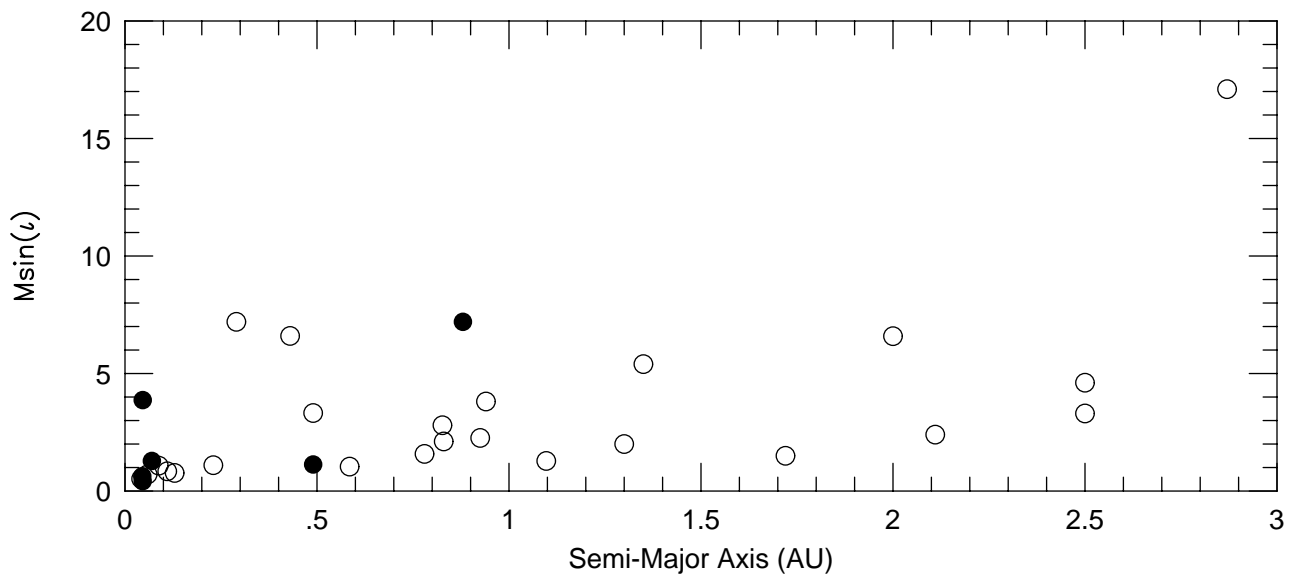


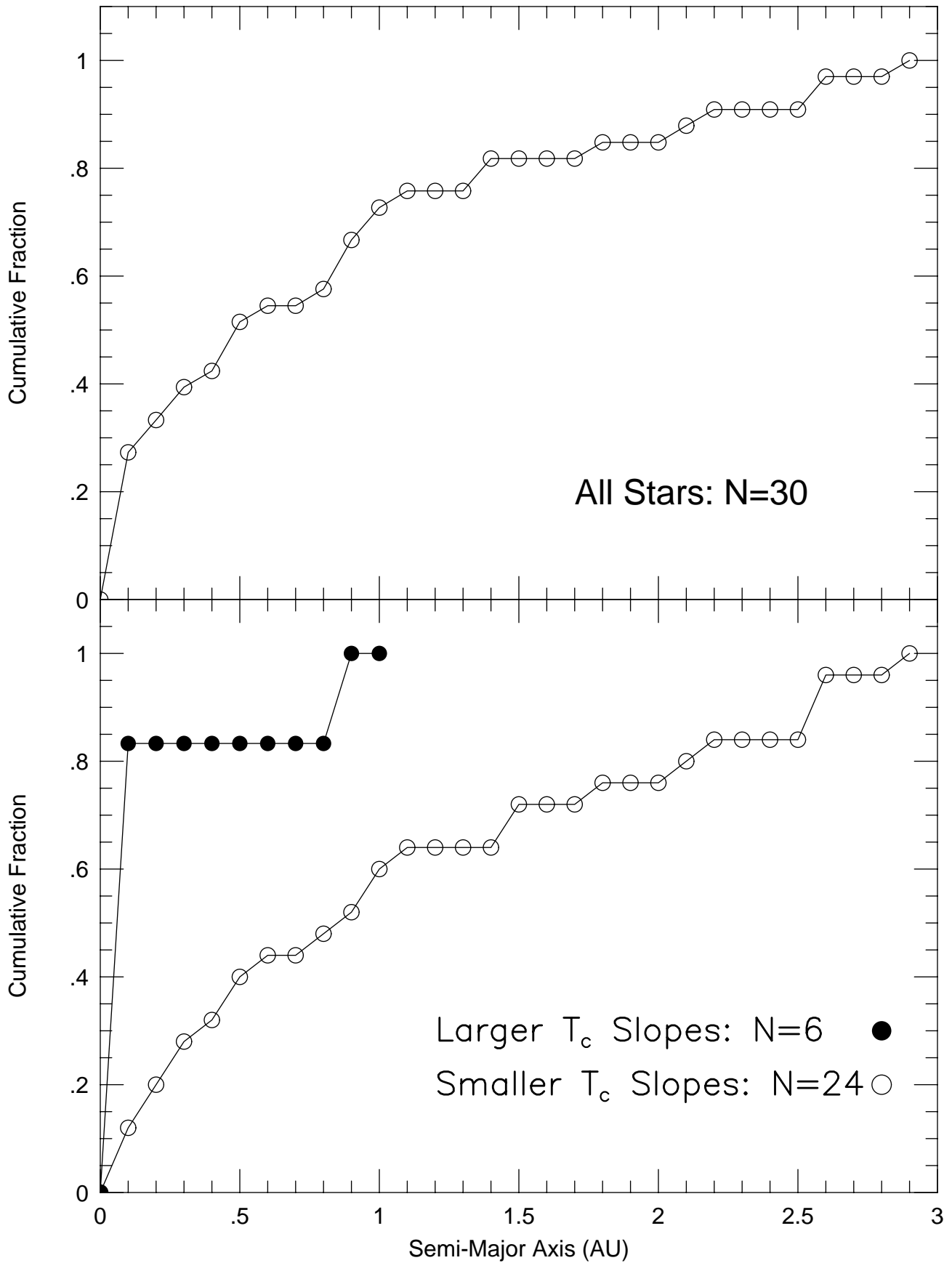












The Abundance Distribution in the Extrasolar-Planet Host Star HD19994

Verne V. Smith

Department of Physics, University of Texas at El Paso, El Paso, TX 79968 USA, and McDonald Observatory, University of Texas at Austin, Austin, TX 78712 USA;
 verne@barium.physics.utep.edu

Katia Cunha

Observatório Nacional, Rua General José Cristino 77, 20921-400 São Cristóvão, RJ, Brazil;
 katia@on.br

Daniela Lazzaro

Observatório Nacional, Rua General José Cristino 77, 20921-400 São Cristóvão, RJ, Brazil;
 lazzaro@on.br

ABSTRACT

Abundances of 22 elements have been determined from a high-resolution, high signal-to-noise spectrum of HD19994, a star recently announced as harboring an extrasolar planet. A detailed spectroscopic analysis of this star finds it to have a mass of $1.2 \pm 0.1 M_{\odot}$. HD19994 is found to be slightly enriched in “metals” relative to the Sun ($[\text{Fe}/\text{H}] = +0.09 \pm 0.05$ and an average of all elements of $[\text{m}/\text{H}] = +0.13$), as are most stars known with extrasolar planets. In an investigative search for possible signatures of accretion of metal-rich gas onto the parent stars in such systems (using HD19994 and published abundances for other stars), it is found that a small subset of stars with planets exhibit a trend of increasing $[\text{X}/\text{H}]$ with increasing condensation temperature for a given element X. This trend may point to the accretion of chemically fractionated solid material into the outer (thin) convection zones of these solar-type stars. It is also found that this small group of stars exhibiting an accretion signature all have large planets orbiting much closer than is found, in general, for stars with planets not showing this peculiar abundance trend, suggesting a physical link between accretion and orbital separation. In addition, the stars showing evidence of fractionated accretion are, on average, of larger mass ($1.2 M_{\odot}$) than stars not showing measurable evidence of this accretion ($1.0 M_{\odot}$).

Subject headings: planetary systems — stars: abundances

1. Introduction

The last five years have been witness to a continuing series of detections of extrasolar planets around solar-type stars using the Doppler method. The number of systems discovered continues to grow, with the current number of solar-type stars known to have planets approaching 50; the first detections were by Mayor & Queloz (1995), Butler & Marcy (1996), and Marcy & Butler (1996), with recent systems being announced by Queloz et al. (2000) and Butler et al. (2000). The current sample of solar-type stars known to harbor planetary systems is biased, of course, by the Doppler method being most sensitive to large planets, as well as large planets that closely orbit their parent stars (neglecting variations in stellar mass, which do not differ greatly over the limited range in spectral type from K to F dwarfs). Thus, the systems detected to date are probably not a representative sample of all planetary systems around solar-type stars. Nonetheless, much can potentially be learned about the formation and evolution of planetary systems by focussing on the detailed properties of the known stars with (large) planets.

One striking property of the stars with planets that have been analyzed spectroscopically to date is their metallicity distribution, where the iron abundance is used typically as a fiducial element with which to define an overall stellar metallicity. As noted first by Gonzalez (1997, 1998), and largely confirmed by continuing work (Gonzalez & Vanture 1998; Gonzalez, Wallerstein, & Saar 1999; Gonzalez & Laws 2000), the Fe abundances in stars with planets tend to be larger than typical values found for field F, G, or K stars not known to have planets. This trend is confirmed most recently in work by Gonzalez et al. (2001) and Santos, Israelian, & Mayor (2001). The differing Fe abundances found between a sample of stars with known (large) planets and a sample of solar-type dwarfs (presumably) more representative of the Galactic disk, suggests that the presence of large planets and Fe abundance, or more generally metallicity, are related. Two possible connections have been discussed: either the presence of planetary systems can influence the metallicity of parent stars or, on the other hand, planets may form preferentially in more metal-rich environments. Discriminating between these two possibilities will help in understanding how systems with large planets form.

In the first case, it is argued that a parent star in a planetary system might accrete chemically fractionated material, depleted in H and He, during early evolution in the system when the star is surrounded by a disk. The mass in the outer convection zone of solar-type stars is relatively small throughout the main-sequence lifetime and material deposited in the envelope can remain there. Accretion of a substantial amount of H- and He-depleted material, relative to the mass in the stellar convection zone, could enhance the metallicity of the outer mass zone of the parent star. The scenario of a young star accreting substantial amounts of material from a protoplanetary disk became a distinct possibility with the discovery of large planets with small orbits, as typified by 51 Peg and τ Boo. It is now suggested (e.g. Lin et al. 1996; Ward 1997; Trilling et al. 1998) that large planets observed close to their parent stars actually formed at larger distances, but migrated inwards due to combinations of drag and/or tidal forces. During inward migration, material from the disk, depleted in H and He, could be accreted onto the star.

Another possibility is that an elevated metal abundance in the natal cloud out of which a star forms might enhance the probability of forming a large planet. According to the standard model (Mizuno 1980; Bodenheimer & Pollack 1986; Pollack et al. 1996; Burrows et al. 1997), the formation of Jovian-mass, or larger, planets is initiated by the condensation of “ices”, such as H₂O or CO₂, thus the primordial abundances of such elements as C or O in the molecular cloud may play a role in large-planet formation.

Quite probably, the processes involved in planet formation are complex, with a number of variables dependent on both primordial abundances and accretion. Detailed chemical abundance analyses of stars known to possess planetary-mass companions will provide useful data in the investigation of how the systems with large planets have formed. In this study, an abundance analysis of 22 elements has been carried out for HD19994 (94 Cet, HR962, HIP14954), which was recently announced by Queloz et al. (2001) to have a planet. This planet has a mass of $M_{\text{psin}\iota} = 2.0M_{\text{Jupiter}}$, orbits with a semi-major axis of 1.3AU, and has a period of 454 days. The chemical abundances in HD19994 are compared to abundances in other planet-harboring stars studied by Gonzalez et al. (2001) and Santos et al. (2001).

2. Observations

The spectrum analyzed here was taken at the University of Texas' McDonald Observatory with the Sandiford cross-dispersed echelle spectrometer, attached to the cassegrain focus of the 2.1m Struve reflector. This spectrometer provides a two-pixel resolving power of $\lambda/\Delta\lambda=R=60,000$ on a 400 x 1200 pixel CCD detector and the spectral coverage for these data were from 6050–7900Å. The star was observed in February 2000. The actual measured resolution achieved in this spectrum of HD19994 was 2.2 pixels (full-width half-maximum), or $R=54,500$.

Data reduction utilized the IRAF software from NOAO. Bias CCD frames were subtracted from the raw program CCD images (star, internal quartz flat-fields, and Th–Ar hollow cathode lamps). The two-dimensional locations of the spectral orders were defined, interorder light was then identified and polynomial fits to this light were made in both the dispersion and cross-dispersion directions, with the resultant interorder light subtracted from the image in question. The bias subtracted and interorder corrected frames were divided by the flat-field images and the defined spectral orders were summed and extracted to obtain a set of one-dimensional spectra. Wavelength calibrations were set from the Th–Ar spectra, with typical residuals from a wavelength fit of 5–8 mÅ. The final signal-to-noise ratio, measured near 6500Å, was $S/N \sim 400$.

3. Analysis

The techniques employed to derive abundances center on using the spectrum to derive the fundamental stellar parameters effective temperature (T_{eff}), surface gravity (parameterized as $\log g$), microturbulent velocity (ξ), and metallicity (characterized by $[\text{Fe}/\text{H}]$). The model atmospheres used in this study were generated with the ATLAS9 code (R. L. Kurucz 1993, private communication). A number of spectral lines, covering as many elements as possible, were analyzed; most lines are largely unblended, so equivalent widths alone are suitable for an abundance analysis. In some instances, however, lines are partially blended and spectrum synthesis was used.

3.1. The Fe I–Fe II Analysis and Stellar Parameters

The neutral and singly ionized iron lines are used to derive basic physical quantities for HD19994. The lines employed are unblended and have accurately measured gf-values. These same lines have been used in recent work by Smith et al. (2000) and the sources of the gf-values are described in more detail there. It is worth noting, however, that the accuracy of most of these oscillator strengths are now at the few percent level (Lambert et al. 1996). Wavelengths, excitation potentials, gf-values, and equivalent widths for HD19994 are listed in Table 1, for 20 Fe I and 4 Fe II lines.

With a set of model atmospheres, Fe abundances can be derived for various T_{eff} 's, gravities, and microturbulent velocities. A simultaneous fit, demanding the same Fe abundance from low- and high-excitation ($\chi \sim 2\text{--}5$ eV) and weak and strong ($\sim 30\text{--}120$ mÅ) Fe I lines, as well as the Fe II lines, yields spectroscopic values of T_{eff} , $\log g$, ξ , and Fe abundance. Figure 1 illustrates part of this process. The slope of Fe-abundance (in units of $\log \epsilon(\text{Fe}) = \log[\text{N}(\text{Fe})/\text{N}(\text{H})] + 12$) versus reduced equivalent-width ($\log W/\lambda$) is plotted on the x-axis, while the slope of $\log \epsilon(\text{Fe})$ versus excitation potential (χ) is plotted on the y-axis. The slopes are derived from a linear least-squares fit to pairs of points of $\log \epsilon(\text{Fe})$ versus either $\log(W/\lambda)$ or χ . Various model atmosphere effective temperatures and microturbulent velocities are shown in Figure 1, with the goal being to achieve no trend of Fe abundance with either χ or $\log(W/\lambda)$, i.e. zero slopes in both axis. The results illustrated are for the sample of Fe I lines and it is clear, that for this gravity ($\log g = 3.95$), $T_{\text{eff}} = 6030\text{K}$ and $\xi = 1.55 \text{ km s}^{-1}$ are the best solution, as indicated by the large filled square at point 0,0. The errorbars shown on this point are derived from the linear least-squares fits to the relations of Fe versus reduced equivalent-width and excitation potential.

In practice, this procedure is done for a variety of $\log g$ values, and at only one particular $\log g$ will the Fe I and Fe II lines yield the same Fe abundances. For HD19994, the value of $\log g$ illustrated in Figure 1 ($\log g = 3.95$) provides the same Fe I and Fe II abundances. The spectroscopically derived best parameters for HD19994 are thus $T_{\text{eff}} = 6030\text{K}$, $\log g = 3.95$, and $\xi = 1.55 \text{ km s}^{-1}$. With such high-S/N spectra as studied here, and a sample of lines with accurate gf-values, an internally consistent set of parameters can be defined with uncertainties of about

± 20 K in T_{eff} , ± 0.05 in $\log g$, and ± 0.05 km s $^{-1}$ in ξ . Of course, there will be systematic effects from both the choice of model atmosphere family and (probably) analysis code, however, these effects are now at about the 0.1 dex level for solar-type stars (with near-solar metallicities), as can be seen by comparisons between various groups studying the same star.

In particular, HD19994 has been analyzed previously and comparisons can be made between the stellar parameters derived from different investigations. From the large abundance study by Edvardsson et al. (1993), this star was found to have $T_{\text{eff}} = 6104$ K, $\log g = 4.10$, and $\xi = 1.85$ km s $^{-1}$. Carretta, Gratton, & Sneden (2000) have also included HD19994 in an abundance analysis of solar-type stars and find $T_{\text{eff}} = 6015$ K, $\log g = 3.94$, and $\xi = 1.47$ km s $^{-1}$. The agreement between the various physical quantities derived for HD19994 from three different studies is very good ($\sigma(T_{\text{eff}}) = 47$ K, $\sigma(\log g) = 0.09$ dex, and $\sigma(\xi) = 0.2$ km s $^{-1}$).

Furthermore, HD19994 is near enough to have a well-defined Hipparcos parallax of $\pi = 44.79 \pm 0.75$ milli-arcseconds, thus, its distance is also known accurately. Given its distance and measured V-magnitude, an absolute visual magnitude can be computed, and, with $T_{\text{eff}} = 6030$ K, the bolometric correction is small so an accurate luminosity can be derived. Given a luminosity, along with the stellar parameters, a stellar mass can be derived from the relation

$$\frac{M_*}{M_{\odot}} = \left(\frac{L_*}{L_{\odot}} \right) \left(\frac{g_*}{g_{\odot}} \right) \left(\frac{T_{\odot}}{T_*} \right)^4,$$

where M , L , g , and T are, respectively, the masses, luminosities, surface gravities, and effective temperatures of the star (*) and Sun (\odot). Table 2 summarizes the physical properties for HD19994: note that we derive a ‘spectroscopic mass’ of $M_* = 1.24M_{\odot}$. Use of the Carretta et al. (2000) stellar parameters (but same L_*) would yield a near-identical mass of $M_* = 1.23M_{\odot}$, while the recent study by Allende-Prieto and Lambert (1999), using Hipparcos parallaxes plus stellar model tracks, finds a mass of $1.28M_{\odot}$ for HD19994: all three of these studies find excellent agreement for the stellar mass. The earlier analysis by Edvardsson et al. (1993), in which HD19994 had a slightly higher T_{eff} and $\log g$, would yield a somewhat higher mass of $1.68M_{\odot}$, which is a bit on the high side for a star classified as an F8V (although the use of the Edvardsson et al. parameters would have only a minor effect on an abundance analysis). Santos, Israelian, & Mayor (2001) have also analyzed HD19994 and their stellar parameters are $T_{\text{eff}} = 6160$ K and $\log g = 4.25$: these are both somewhat larger values than those derived by the studies mentioned above. Use of these particular values for effective temperature and gravity, along with the luminosity derived from the Hipparcos parallax (the relatively small differences in T_{eff} from the above studies will lead to negligible differences in any bolometric corrections), would yield a mass of $2.3M_{\odot}$ for HD19994: this is much too large for its spectral type (F8V). Both a larger T_{eff} and $\log g$ will lead to, typically, larger derived abundances, so it is no surprise that Santos et al. (2001) measure somewhat larger abundances ($[\text{Fe}/\text{H}] = +0.23$). Most of the more recent studies described above, however, indicate that the parameters for HD19994 are secure and that an accurate abundance analysis can be conducted on this star.

With a relatively well-defined T_{eff} and luminosity, the mass of HD19994 can also be estimated

from stellar evolutionary model tracks. Using the stellar models from Schaerer et al. (1993), with $Z=0.02$ (as HD19994 is only modestly enhanced in metals with respect to the Sun) we derive a mass for HD19994 of $1.3M_{\odot}$ and an age of 4.3Gyr, quite close to the age of the Sun and solar system.

3.2. Abundances Other Than Fe

There are 21 elements, other than Fe, which have lines analyzed in this spectrum of HD19994 (including boron which was analyzed by Cunha et al. 2000 using HST UV-spectra). Table 3 contains the line identifications, wavelengths, excitation potentials, gf-values, and measured equivalent widths in HD19994. The sources of the gf-values are taken either from Smith et al. (2000), who employed a very similar set of lines in an analysis of globular cluster giants using red spectra, or from Gonzalez et al. (2001), who provide a large compendium of abundances derived for stars with extrasolar planets. Both studies provide details about the gf-values, with most of the Smith et al. oscillator strengths being measured values taken from the literature (with a few solar values derived from a solar model generated with the MARCS code), while the Gonzalez et al. gf-values are solar ones, derived from an analysis of a reflected solar spectrum (Vesta) using a Kurucz ATLAS9 solar model. Differences between the solar gf-values derived from Smith et al. and Gonzalez et al. solar analyses are small.

Some elements required spectrum synthesis, thus to both illustrate this method of deriving abundances, as well as to demonstrate the overall quality of the spectra, Figure 2 shows two regions which were synthesized in HD19994. The [O I] line near 6300Å and the Li I line near 6707Å are shown, with the filled circles being the observed data points and the solid curves the synthetic spectra. Note the telluric O₂ line near the 6300Å [O I] line: rapidly-rotating hot-stars are observed to provide templates to map the telluric lines and can be used to ratio out the O₂ lines, however, if the telluric lines do not interfere with fitting the [O I] feature, no ratioing is done, as is the case here.

In this study a direct abundance comparison is made between the Sun and HD19994. Abundances are derived from the same sets of lines as those used for HD19994 and the final elemental abundances found for HD19994 are then ratioed to their respective solar values and abundances are then presented as [X/H]. Final abundances are listed in Table 4. The solar equivalent-widths (or spectra for spectrum synthesis) were measured from the solar flux atlas of Kurucz et al. (1984) and the lines analyzed using an ATLAS9 model with $T_{\text{eff}}=5777\text{K}$, $\log g=4.43$, and $\xi=1.0 \text{ km s}^{-1}$ (as derived from this set of Fe I lines). The differences between the abundances derived here for the Sun and the accepted photospheric values (e.g. Grevesse et al. 1996) are small. (See discussion in Smith et al. 2000).

Values of the abundances in HD19994, relative to the Sun, as [X/H] are plotted in Figure 3. The 22 elements studied here range in mass from Li, B, or C, up to Eu and span a range

in nucleosynthetic origins. Other than a general overabundance of +0.13 dex in HD19994 (as indicated by the solid horizontal line, with the solar ratio of $[X/H]=0.0$ shown by the horizontal dashed line), no other trends are apparent in this figure. This star does continue the tendency, however, of planet-bearing stars being metal-rich. Although not “super-metal rich”, which is defined to be at least +0.2 dex enriched, relative to the Sun, HD19994 is more metal-rich than the Sun and is near the peak of the metallicity distribution found for the stars with planets. The abundance of $[Li/H]$ is not plotted in Figure 3 as this element is very sensitive to stellar mixing processes and the abundance of $\log \epsilon(Li) = 1.81$ is not unusual for a late-F dwarf.

4. Discussion

Two aspects of the abundances in HD19994 will be discussed here: are there overall abundance signatures in the stars with large planets compared to stars not known to have large planets, and are there any indications of chemical fractionation occurring in possible accretion processes in stars with large planets.

4.1. Abundance Ratios in HD19994 Compared to Stars with Large Planets and Field Stars

As pointed out in the Introduction, most abundance studies of stars with large planets have found that these stars tend to have rather high metallicities: the most recent papers and summaries of work are by Gonzalez et al. (2001) and Santos et al. (2001). In the top panel of Figure 4 are shown the Fe-abundance distributions for a volume-limited sample of solar-type stars, along with the same distribution for the known stars with planets that have been spectroscopically analyzed for their Fe abundances. The volume-limited sample is from Favata et al. (1997), while the planet-harboring stars are taken from Gonzalez et al. (2001) and Santos et al. (2001). These two studies include results for 30 stars, but we show in Figure 4 only those stars for which oxygen abundances have also been determined (26 stars). The arrow shows the $[Fe/H]$ abundance for HD19994, which is near the peak of the distribution for planet-bearing stars. To date, the parent stars with planets exhibit a distribution of Fe abundances skewed strongly towards larger $[Fe/H]$ values. Since these two separate stellar samples have not been chosen in the same way, there is the possibility of selection effects that are not understood playing a role in the $[Fe/H]$ distributions for the stars with planets. Nonetheless, the relatively large metallicities found for the planet-hosting stars are interesting and the detailed abundance distributions in these stars warrant a closer look.

The distribution of $[O/H]$ abundances for planet-hosting stars is shown in the bottom panel of Figure 4 (no such volume-limited distribution exists for field solar-type stars). Most of these oxygen abundances are corrected values taken from the Gonzalez et al. (2001) study, and were obtained from the IR O I triplet lines at 7774Å. These particular O I lines are quite strong and

may suffer from non-LTE or granulation effects. Edvardsson et al. (1993), in a large study of F and G stars, compared LTE oxygen abundances derived from both the [O I] 6300Å line (which forms in LTE) and the O I 7774Å lines. They determined empirical corrections that can be applied to the 7774Å O I abundances to bring them into agreement with the [O I] 6300Å line; this correction is valid for the stellar parameters spanned by the stars with planets studied by Gonzalez et al. Thus, the O abundances shown in the bottom panel of Figure 4 are derived from the LTE 7774Å abundances, with the Edvardsson et al. correction applied to them. The [O/H] abundance distribution is shifted slightly towards smaller values than those for [Fe/H] by about 0.1 dex, with a somewhat larger fraction of stars with $[O/H] \leq 0.0$. Oxygen is shown as a comparison to iron because, as discussed in the Introduction, the abundance of O may play an important role in large-planet formation.

Comparisons of strategic abundance ratios are shown in Figures 5, 6, and 7 for various samples of field solar-type stars, plus HD19994, and other stars with planets. Both Gonzalez et al. (2001) and Santos et al. (2001) have previously conducted such a comparison, however, here we select slightly different field-star samples as comparisons, as well as add HD19994, and use oxygen as the fiducial metallicity indicator instead of iron. Oxygen abundances are somewhat more difficult to measure than iron, with fewer O I lines than Fe I and Fe II, and with the stronger O I lines suffering from possible non-LTE effects (such as the O I 7774Å triplet). Although free from non-LTE effects, the [O I] 6300Å is quite weak and requires spectra of rather high-S/N. Oxygen is, however, a superior monitor of metallicity in stars with planets as it is not only the most abundant element after H and He, but also plays a major role in the formation of large planets, as these planets form initially around icy cores, where H₂O and CO₂ dominate. Figure 5 compares the [O/Fe] ratios, versus [O/H], for known stars with planets and a series of field-star samples of F, G, and K dwarfs. As discussed above, the O abundances for the Gonzalez et al. stars are LTE abundances derived from the 7774Å O I lines, with the empirical corrections derived by Edvardsson et al. (1993) applied to them. The other studies shown in Figure 5 either rely directly on the [O I] 6300Å line (which is a first class abundance indicator [Lambert 1978]), or use the O I 7774Å lines with non-LTE or empirical corrections ,e.g. Edvardsson et al. (1993), applied to the LTE abundances. No large differences exist between the various investigators in the adoption of stellar parameters for near-solar metallicity solar-type stars, thus all of the abundances shown in Figure 5 should be on nearly the same scale. This is born out by the large degree of overlap between the different studies, and no apparent significant offsets.

There is nothing remarkable in Figure 5, except to note how well the stars with planets fit into the overall trends of the field stars. Above a metallicity of ~ 0.15 in [O/H], both the field stars and stars with planets show a rather flat run of [O/H], with small scatter for most stars ($\sim \pm 0.1$ dex). Below this value of [O/H], the well-known increase in [O/Fe] with decreasing metallicity is apparent, again, with most stars showing only small scatter from a mean trend. Note that in the distribution of [O/Fe] versus [O/H] in Figure 5, there is a fairly well-defined lower envelope, with only a few outliers, however, there are conspicuous numbers of stars falling above the mean trend

(i.e. large values of $[O/Fe]$ for a given $[Fe/H]$). Feltzing & Gustafsson’s (1998) sample contains the largest fraction of these stars (and they specifically concentrated on metal-rich stars), although all studies show some stars in this region of the diagram. By-and-large, however, the stars with large planets do not stand out from the field distribution, except tending to fall towards the high-metallicity end (as already discussed). HD19994 falls near the middle of the distribution of $[O/Fe]$ and $[O/H]$ abundances, and appears normal in this regard.

Another crucial element in the formation of ices in protoplanetary disks is carbon, and comparisons using this element as a basis are shown in Figure 6. The top panel is $[C/Fe]$ versus $[O/H]$ while the bottom panel is the ratio $[C/O]$ versus $[O/H]$. Field-star samples with both C and O are more limited than many other elements and the comparison sample here consists of C abundances from Tomkin et al. (1995) combined with O abundances in those same stars from Edvardsson et al. (1993). Tomkin et al. adopted the same stellar parameters as Edvardsson et al., so these two studies should be self-consistent. In addition, Tomkin et al. used the C I lines near 7110Å with many of the C abundances for the stars with planets being derived from these same lines (as well as in HD19994), thus there do not appear to be any offsets between the field star sample of stars not known to have planets and those stars known to have planets. Although there are fewer field comparison stars, there again appears to be nothing dramatic in a comparison of carbon in stars known to have large planets, and those not known; HD19994 falls near the upper envelope in both plots of the stars with planets, indicative of a very slightly larger C abundance, but not significantly so.

Finally, in Figure 7, the elements Na and Al are included in a comparison. Of all the elements analyzed by Gonzalez et al. (2001), they found a hint that Na might be slightly lower in the stars with large planets. The top panel of Figure 8 shows $[O/Na]$ versus $[O/H]$ and there is a small subset of the stars with planets that falls above the trend of $[O/Na]$ versus $[O/H]$ as defined by the Edvardsson et al. (1993), Feltzing & Gustafsson (1998) and Carretta et al. (2000) field-star results. All of these various studies use some combination of the same Na I lines near 5685Å or 6155Å and the different samples of abundances all overlap to a large degree: there are no significant offsets from one study to the next.

The modest enhancement of $[O/Na]$ in some of the stars with planets is a combination of slightly larger oxygen and slightly lower Na abundances. Remarkably, many of the Feltzing & Gustafsson stars (which were chosen to be of high metallicity) fall within this small grouping. HD19994 falls near the low end of $[O/Na]$ for the stars with planets, but near the middle of the main trend in the field star samples. We thus confirm the tentative conclusion from Gonzalez et al. that there are a sizable fraction of stars with large planets that have slightly lower Na abundances (and this result is strengthened by the fact that they used Fe as the fiducial comparison element while we use O). A plot of $[Na/Al]$, however, in the bottom panel of Figure 7 shows that the stars with planets fall right within the scatter of field stars from Edvardsson et al. (1993) and Feltzing & Gustafsson (1998).

4.2. Is There Evidence of Chemical Fractionation?

Besides comparing overall abundance trends in stars with large planets versus samples of stars not known to have planets, internal abundance distributions can be a useful, and potentially more sensitive, diagnostic. As mentioned in the Introduction, one possible explanation for the large metallicities found in stars with large planets is that the parent stars accreted some material, depleted in H and He, from the disk out of which the planets formed. Gonzalez et al. (2001) and Santos et al. (2001) reach different conclusions concerning evidence for this accretion scenario. Santos et al. find no trends of [Fe/H] versus stellar convective envelope mass and conclude that accretion of fractionated material is not enough to significantly affect the metallicities. Gonzalez et al., on the other hand, suggest that accretion may play a role in the observed [Fe/H] distribution. A recent study by Laws & Gonzalez (2001) of 16 Cyg A and B finds small, but significant, differences in [Fe/H] for the two members of this binary system, as well as a large difference in their respective Li abundances. They suggest that these abundance differences could be due to the accretion of planetary material by 16 Cyg A, resulting in its somewhat larger [Fe/H] and [Li/H] values relative to 16 Cyg B.

An investigation into possible accretion can be probed further by searching for abundance patterns that depend upon elemental condensation temperature, T_c . If solid material is accreted by a star, in quantity, the accretion might possibly occur in a rather high temperature environment (i.e. close to the star). In such a situation, refractory elements might be added preferentially when compared to volatile elements. This idea was explored initially by Gonzalez (1997) in an abundance analysis of ν And and τ Boo. Gonzalez also searched for possible evidence of a fractionation pattern in the Sun by comparing differences between solar photospheric and meteoritic abundances as a function of elemental condensation temperature, but did not detect a significant signature. In Figure 8 the abundances in HD19994 are plotted versus the elemental condensation temperature, with T_c taken from Lodder & Fegley's (1998) table of T_c 's for a solar composition at a pressure of 10^{-3} bar. Changing the conditions will change the absolute values of T_c , but not the relative order of the elements as shown in Figure 8. If significant accretion of material depleted in H and He occurred, there might also be other fractionation patterns in the accreted matter. In such a case, trends might be detectable in the abundances as a function of T_c ; in the case of HD19994 (Figure 8), no such trend is apparent. A trend in [X/H] versus T_c can be quantified by a single number if a straight line is fit to the abundance versus condensation temperature points. The appearance, or lack, of a slope in such a plot does not involve any physical arguments about whether accretion of fractionated material should necessarily produce a linear trend, but is simply a way of quantifying the abundance distribution with T_c and comparing different stars. A linear least-squares fit to such a plot for HD19994 finds an insignificant negative slope of $-6.1(\pm 9.8)\times 10^{-6}$ dex/K, indicating no measurable trend whatsoever. If material was accreted by HD19994 it was only depleted measurably in H (and probably He).

In this paper, the same type of analysis, looking for fractionation patterns, was also carried out for the abundances presented by Gonzalez et al. (2001), where typically 15 elements were analyzed,

including such elements as C and O, which have low T_c , S and Na which have intermediate condensation temperatures, and Fe, Ti, or Al, which have fairly high values of T_c . The derived slopes are illustrated graphically in Figure 9, along with the result for HD19994 obtained here. The abundance work by Santos et al. (2001) does not contain such a large number of elements, so his distributions are not used in this sample comparison; the more elements sampled, and the wider the range in T_c , lead to more constrained slopes in $[X/H]$ versus T_c . The average of the Gonzalez et al. slopes is shown by the vertical dashed line, with plus and minus one standard deviation lines also shown, and there is a small positive offset from slope zero. Five stars stand out in Figure 9, with the largest positive slopes of $[X/H]$ with T_c : these stars are HD52265, HD75289, HD89744, HD209458, and HD217107. The slopes are such that low condensation species, such as C, N, or O, are ~ 0.2 dex lower in abundance than the more refractory species, such as Ti, Sc, or Al. These stars are prime candidates for possibly having accreted substantially fractionated material and additional, detailed abundance analyses of these stars are encouraged. The star with the most negative slope in Figure 9 is HD37124, which also has the lowest iron abundance with $[Fe/H] = -0.41$, while the star with the next lowest slope is HD46375, also has a relatively low metallicity ($[Fe/H] = -0.03$) for this sample of stars. The lower slopes associated with lower values of $[Fe/H]$ suggests that there are chemical evolutionary effects, which are not related at all with fractionation, and must be investigated.

In order to probe the effects of chemical evolution on fitting slopes to $[X/H]$ versus T_c , two samples of field stars, which covered a wide range of elements, were used: Edvardsson et al. (1993) and Feltzing & Gustafsson (1998). Disk chemical evolutionary effects are illustrated in Figure 10, where the parameterized slopes are plotted versus $[Fe/H]$. The stars from Edvardsson et al. (1993) and Feltzing and Gustafsson (1998) that are used as “control” samples with which to see effects from general chemical evolution are plotted as open symbols in Figure 10 and identified as BDP (for Big Disk Paper) and FG (Feltzing & Gustafsson). Stars from Gonzalez et al. (2001), as well as HD19994, are shown as filled circles. Error bars reflect the statistical uncertainty in the derived slopes, with assumed abundance errors of 0.10 dex in $[X/H]$. All three samples of stars use somewhat different mixtures of elements, which could lead to small systematic differences in the derived T_c slopes. There is a large overlap, however, in the derived slopes from all samples, and the three studies all include elements with a broad range of condensation temperatures (especially O). The large degree of overlap suggests that any systematic effects between the studies are smaller than the scatter.

Concentrating on the BDP and FG points, there is a clear trend of a decreasing slope in $[X/H]$ versus T_c as $[Fe/H]$ decreases: this is the signature of Galactic chemical evolution in this diagram and not an indication of chemical fractionation. In these data, oxygen is one of the most volatile species included, and carries a great deal of weight in defining the slopes; as $[O/Fe]$ rises towards lower metallicities, it tends to produce a negative slope in a plot of $[X/H]$ versus T_c . A straight line through the BDP points is shown to illustrate the general trend in the field stars. As the abundances used in the analyses are all relative to the Sun, the fitted straight line

goes nearly through the zero-zero point as it should. In general, the stars with large planets show a remarkable overlap with the general field samples: most of the stars with planets fall within the scatter of the BDP and FG results, suggesting no measurable differences in the overall abundance distributions with condensation temperature at a given $[\text{Fe}/\text{H}]$. Of course, not all of the Edvardsson et al. and Feltzing and Gustafsson stars have been searched for large planets, and there remains the possibility that fractionation effects lie in small numbers of stars in both samples. To search for selective accretion of refractory species, the target stars should have large positive slopes, and there is such a small subset of 5-6 stars in Figure 10 that cluster at larger $[\text{Fe}/\text{H}]$ and fall above the general scatter: these include the same 5 stars noted from Figure 9. These stars show an abundance pattern not seen in the other stars due to general, overall chemical evolution of the Galaxy. A total of 6 stars stand out from combining results from both Figure 9 and 10 as having slopes well above the mean trend: these stars are HD52265, HD75289, HD89744, HD120136, HD209458, and HD217107. Abundances as a function of T_c are shown for two stars from this group (HD75289 and HD209458) in Figure 11. As discussed previously, the straight-line fits to the abundances are not met to imply that there is a real linear relation between $[\text{X}/\text{H}]$ and T_c , but are used to characterize the abundance distribution by a single number (the slope). Both stars exhibit a pattern in which the more volatile elements (C, N, O, S, and Zn) are ~ 0.3 dex lower in abundance than the more refractory elements (Si, Ti, Ca, and Sc). This is clearly not the definitive study, as a detailed, uniform analysis must be applied to samples of stars with planets and stars known not to have large planets, yet the stars noted above should be subjected to very careful abundance analyses, as they exhibit the clearest signatures of potential accretion of fractionated material. Note that two of the Feltzing & Gustafsson (1998) stars also fall within this selective group (this is about 10% of the FG stars plotted here and we only used those FG stars in which they determined O abundances): HD110010 and HD137510 (these stars should be prime candidates for having closely orbiting planets). This percentage of stars in the FG sample that might have planets is in approximate agreement with the recent study by Laughlin (2000), who argues that $\sim 10\%$ of solar-type field stars with $[\text{Fe}/\text{H}] \geq +0.2$ might have large planets.

Other than larger than normal slopes in plots of $[\text{X}/\text{H}]$ versus T_c , do the abovementioned stars exhibit any other distinctive properties? Physical parameters of the detected planets in extra-solar systems are shown in three panels of Figure 12, with the stars with the larger T_c slopes plotted as filled circles. In the top two panels of Figure 12, the companion masses ($M \sin(\iota)$) are plotted versus eccentricity (e) and semi-major axis (a): the stars with possible accretion signatures stand out as having smaller orbital separations, as well as possibly somewhat smaller eccentricities and companion masses (although the masses are only lower limits, as the inclinations are not, in general, known). In the bottom panel the eccentricities and semi-major axes are compared, and the stars showing accretion evidence are well segregated to the small e , small a part of this plot.

A striking difference between the stars with the largest T_c -slopes and the others can be seen in the respective distributions of their companion's semi-major axes. Figure 13 shows cumulative fractional distributions of the values of a (with the cumulative fraction being the fraction of stars

in that sample having companions which have a less than a particular value). In the top panel, the entire sample of 30 stars is shown, while in the bottom panel, the sample is divided into the 6 stars falling furthest from the general trend of T_c -slope versus [Fe/H] (filled circles), and the other 24 (open circles). The stars showing the most evidence of possible fractionated accretion are biased strongly towards having close companions and the two distributions are clearly different. Could these two differing distributions be caused by random sampling? As a check on this, random 6-point samplings of the entire 30-point data set were conducted and subsequent cumulative fractional distributions were computed for each random set. Doing this exercise 5000 times it was found that a cumulative fractional distribution rising as rapidly as that found for the 6 stars with the large T_c -slopes occurs only 5% of the time. It is unlikely that the observed distribution has arisen by chance; there is a link between the abundance distributions and small separations of large planets.

The “dynamical” properties of the orbits are completely independent from abundance analyses and suggest that there must be a physical process at work here. Lower eccentricities may be a fossil signature of a protoplanetary disk, as small eccentricities are a requirement of the standard model for giant-planet formation, resulting from the gradual accretion of small solid particles in a disk, followed by gravitational accretion of gas. Smaller orbital separations suggest the possibility of more interaction between planet, disk, and star, as the planet presumably migrated inwards to its current position around its parent star when it was forming. It is worth noting that among the stars which exhibit signatures of fractionated accretion is HD209458. This star has the only companion whose mass has been well-determined by transit observations: $M_{\text{comp}} = 0.63M_J$ (Charbonneau et al. 2000). This mass definitely classifies it as a planet, well below the deuterium-burning limit.

Another property of the stars that can be examined is their mass. Again, the six star-planet systems with the largest slopes of [X/H] versus T_c are somewhat distinctive relative to the other star-planet systems. The 24 systems that do not exhibit T_c slopes noticeably different from field-star samples of stars not known to have planets have a mean stellar mass of $1.06M_{\odot}$ (with a standard deviation of $0.12M_{\odot}$), while the 6 stars exhibiting the largest T_c slopes have a mean mass of $1.23M_{\odot}$ (with a standard deviation of $0.17M_{\odot}$). These mass estimates are taken from the papers by Gonzalez et al. (2001) and Santos et al. (2001) and have been estimated using stellar evolutionary tracks. The suggestive link here would be that the more massive stars have smaller mass convective envelopes and would thus be easier to pollute with accreted material. It is worth noting that, for an age of 10^8 years and models from D’Antona & Mazzitelli (1994), the convective envelope mass goes to near-zero above a mass of $\sim 1.15M_{\odot}$ and 5 of the 6 stars with significant T_c slopes lie above this limit. The one exception is HD217107, which is estimated to have a mass of $0.98M_{\odot}$, however, there are at least $0.1M_{\odot}$ uncertainties in all of these estimates. There are two systems that do have high masses and closely orbiting planets, but do not show any trend of [X/H] with condensation temperature: HD9826 and HD38529. Both of these systems have their own unique properties within this sample. HD9826, with a mass of $1.3M_{\odot}$, has three large planets

with semi-major axes ranging from 0.05 to 2.5AU, with the two outer planets in eccentric orbits; the dynamical history of this system could be quite complex. With a mass of $1.5M_{\odot}$, HD38529 has one of the largest masses in the sample and has a planet at a distance of 0.13AU, however, it is also one of the most highly evolved stars in the sample. It lies well above the main-sequence, by ~ 1 magnitude, so if it had accreted any material early in its history, a combination of a deepening convective envelope and possible mass loss could have erased a thin veneer of accreted matter.

Because the data used to obtain the slopes illustrated in Figure 9 are quite heterogeneous, definitive conclusions must await further observations; the prime motivation here is to draw attention to these stars. Within this sample, those stars with the largest positive slopes of [X/H] versus T_c tend to have giant planets in near-circular orbits well within 1AU. Further detailed abundance analyses of these stars are in order, as well as results for more stars which have been observed and found not to have large planets in close orbits as a comparison sample. Elements having low- to intermediate-condensation temperatures, such as S, Cu, or Zn should be included in the analyses, as well as the abundant trio C, N, and O.

5. Conclusions

An abundance analysis covering some 22 elements has been presented for HD19994, another star now known to harbor a large planet. As found in previous studies, e.g. Gonzalez et al. (2001) or Santos et al. (2001), where the stars with large planets tend to be metal-rich, HD19994 is slightly metal-rich, with $[Fe/H] = +0.09 \pm 0.05$. An average of all 22 elements finds $[X/H] = +0.13$. No obvious trends of nuclear origin are found in the abundances of HD19994, nor is there a trend with elemental condensation temperature, which might occur if the star had accreted substantial amounts of chemically fractionated material from a protoplanetary disk. A comparison of the abundance distributions versus T_c in the sample of stars with planets from Gonzalez et al. (2001) finds 6 stars which are the most likely candidates for having possibly accreted fractionated material. It is also found that these 6 candidate stars share the dynamical system property of having quite small orbital separations. In addition, these 6 stars tend to be the more massive stars known to have planets. Continuing abundance analyses of a broad range of elements in all stars known to have planets, compared to a sample of stars known not to have large planets, will shed light on whether the formation of large planets can measurably alter the apparent metallicities of their parent stars. In addition, such work will help determine whether the formation of large planets is more likely to occur in a metal-rich environment.

We thank the staff of McDonald Observatory. The referee, Guillermo Gonzalez, is to be thanked for providing a careful reading of the initial paper and for suggesting some useful comments which improved the final version. This research is supported in part by the National Science Foundation (AST99-87374).

REFERENCES

Allende Prieto, C., &, Lambert, D.L. 1999, A&A, 352, 555

Bodenheimer, P. & Pollack, J. B. 1986, Icarus, 67, 391

Burrows, A., Marley, M., Hubbard, W. B., Lunine, J. I., Guillot, T., Sumon, D., Freedman, R., Sudarsky, D., & Sharp, C. 1997, ApJ, 491, 856

Butler, R. P., & Marcy, G. W. 1996, ApJL, 464, L153

Butler, R. P., Vogt, S. S., Marcy, G. W., Fisher, D. A., Henry, G. W., & Apps, K. 2000, ApJ, 545, 504

Carretta, E., Gratton, R.G., & Sneden, C. 2000, 356, 238

Charbonneau, D., Brown, T. M., Latham, D. W., & Mayor, M. 2000,

Cunha, K., Smith, V. V. & Lambert, D. L. 1998, ApJ, 493, 195

Cunha, K., Smith, V. V., Boesgaard, A. M., & Lambert, D. L. 2000 ApJ, 530, 948

D'Antona, F., & Mazzitelli, I. 1994, ApJS, 90, 467

Edvardsson, B., Andersen, J., Gustafsson, B., Lambert, D. L., Nissen, P. E., & Tomkin, J. 1993, A&A, 275, 101

Favata, F., Micela, G., & Sciortino, S. 1997, A&A, 323, 809

Feltzing, S., & Gustafsson, B. 1998, A&AS, 129, 237

Gonzalez, G. 1997, MNRAS, 285, 403

Gonzalez, G. 1998, A&A, 334, 221

Gonzalez, G., & Vanture, A.D. 1998 A&A, 339, L29

Gonzalez, G., Wallerstein, G., & Saar, S.H. 1999 ApJ, 511, L111

Gonzalez, G., & Laws, C. 2000 AJ, 119, 390

Gonzalez, G., Laws, C., Tyagi, S., & Reddy, B.E. 2001, AJ, 121, 432

Grevesse, N., Noels, A., & Sauval, A. J. 1996, in Cosmic Abundances (ASP Conf. Ser. Vol. 99), eds. S. S. Holt & G. Sonneborn (San Francisco: Astron. Soc. Pac.), p.117

Kurucz, R.L., Furenlid, I., Brault, J., & Testerman, L. 1984, Solar Flux Atlas from 296 to 1300nm (Cambridge: Harvard Univ. Press)

Lambert, D.L. 1978, MNRAS, 182, 249

Lambert, D.L., Heath, J.E., Lemke, M., & Drake, J. 1996, *ApJS*, 103, 183

Laughlin, G. 2000, *ApJ*, 545, 1064

Laws, C., & Gonzalez, G. 2001, *ApJ*, in press (astro-ph/0101304)

Lin, D. N. C., Bodenheimer, P., & Richardson, D. C. 1996, *Nature*, 380, 606

Lodders, K., & Fegley, B. 1998, in *The Planetary Scientist's Companion* (New York: Oxford University Press)

Marcy, G. W., & Butler, R. P. 1996, *ApJL*, 464, L147

Mayor, M., & Queloz, D. 1995, *Nature*, 378, 355

Mizuno, H. 1980, *Prog. Theor. Phys.*, 64, 544

Nissen, P. E., & Edvardsson, B. 1992, *A&A*, 261, 255

Pollack, J. B., Hubickyj, O., Bodenheimer, P., Lissauer, J. J., Podolak, M., & Greenzweig, Y. 1996, *Icarus*, 124, 62

Queloz, D., Mayor, M., Weber, L., Blecha, A., Burnet, M., Confino, B., Naef, D., Pepe, F., Santos, N., & Udry, S. 2000, *A&A*, 354, 99

Queloz, D., Mayor, M., Naef, D., Pepe, F., Santos, N.C., Udry, S., & Burnet, M. 2001, in *Planetary Systems in the Universe: Observation, Formation and Evolution*, ASP Conf. Ser., eds. A.J. Penny, P. Artymovics., A.M. Lagrange, & S.S. Russell

Santos, N.C., Israeli, G., & Mayor, M. 2001a, *A&A*, 363, 228

Santos, N.C., Israeli, G., & Mayor, M. 2001b, in *Planetary Systems in the Universe: Observation, Formation and Evolution*, ASP Conf. Ser., eds. A.J. Penny, P. Artymovics, A.M. Lagrange, & S.S. Russell

Schaerer, D., Charbonnel, C., Meynet, G., Maeder, A., & Schaller, G. 1993, *A&AS*, 102, 339

Smith, V.V., Suntzeff, N.B., Cunha, K., Gallino, R., Busso, M., Lambert, D.L., & Straniero, O. 2000, *AJ*, 119, 1239

Takeda, Y. 1994, *PASJ*, 46, 53

Tomkin, J., Woolf, V. M., Lambert, D. L., & Lemke, M. 1995, *AJ*, 109, 2204

Trilling, D. E., Benz, W., Guillot, T., Lunine, J. I., Hubbard, W. B., & Burrows, A. 1998, *ApJ*, 500, 428

Ward, W. R. 1997, *Icarus*, 126, 261

Fig. 1.— An illustration of the derivation of the fundamental stellar parameters T_{eff} , $\log g$, and microturbulence (ξ). The slope of $\log \epsilon(\text{Fe I})$ versus excitation potential (χ) is shown as a function of the slope of $\log \epsilon(\text{Fe I})$ versus $\log(W/\lambda)$; zero slopes in both axes indicates the best values of T_{eff} and ξ (identified by the filled square). Differing model effective temperatures and microturbulent velocities are shown by the connected curves, with all of this illustrated for a single model surface gravity ($\log g = 3.95$). Singly ionized iron, Fe II, is most sensitive to $\log g$, and the procedure shown is carried out for a range of values of $\log g$. The example shown here of $\log g = 3.95$ yields the same Fe I and Fe II abundances for the best values of T_{eff} and ξ .

Fig. 2.— Sample observed and synthetic spectra for two small regions in HD19994. Two weak features used for deriving abundances are shown, with [O I] 6300Å in the top panel and Li I 6707Å in the bottom panel. Three different O and Li abundances are shown for each set of synthetic spectra in each panel, respectively, as well as syntheses with no O (top) and no Li (bottom). Extra broadening (beyond instrumental) was required to fit the line shapes in HD19994, with a typical velocity width of 6 km s⁻¹ needed; at this spectral resolution, it is not possible to decompose this broadening into macroturbulence plus rotation. Note the telluric O₂ line in the 6300Å region, which was not removed as it had no effect on the [O I] fits.

Fig. 3.— Abundances in HD19994 as a function of element number, with values plotted as [X/H] relative to solar. A solar abundance ratio is indicated by the horizontal dashed line ([X/H] = 0.0), while the solid horizontal line is the average value in HD19994 for all elements shown ([X/H] = +0.13).

Fig. 4.— Iron and oxygen abundance frequency distributions for a sample of solar-type stars and stars with planets. The top panel shows [Fe/H] distributions for a volume-limited sample of stars from Favata et al. (1997) and a sample of stars with planets from Gonzalez et al. (2001), Santos (2001), and HD19994 from this study (the arrows indicate the abundances for HD19994). Only the stars with planets that have also had oxygen abundances measured are plotted. The Fe distribution of the stars with planets is skewed strongly towards rather large values of [Fe/H]. The bottom panel shows [O/H] for the same planet-harboring stars from the top panel (no volume-limited sample of field stars with O abundances exists). The [O/H] distribution is slightly different than [Fe/H], being shifted somewhat (~ 0.1 dex) to lower values.

Fig. 5.— The behavior of [O/Fe] with [O/H] (“metallicity”) in several solar-type stars, including stars with planets. The general trend of Galactic disk chemical evolution is visible, with [O/Fe] being relatively flat from [O/H] ~ -0.15 to $+0.20$, and increasing below [O/H] = -0.20 . The distributions of the various field-star samples overlap very well. In general, the stars with planets do not noticeably segregate from the general population of field stars.

Fig. 6.— Comparisons of [C/Fe] and [C/O] as a function of [O/H]. The stars with planets do not stand out noticeably from the field F and G stars with measured C and O abundances.

Fig. 7.— Na and Al are compared to O in stars with planets and a number of other field-star

studies. As discerned by Gonzalez et al. (2001), a small group of stars with planets stand out as having somewhat larger [O/Na] ratios at high values of [O/H]. A substantial fraction of the high-metallicity Feltzing and Gustafsson (1998) sample also fall in this region. In terms of [Na/Al] ratios, the stars with planets fall right within the field-star trends with little scatter.

Fig. 8.— Abundances, relative to solar, in HD19994 plotted versus the elemental condensation temperature, T_c . Values for T_c are taken from Lodders & Fegley (1998), and the elemental names are indicated. No trend of [X/H] with T_c exists in HD19994, indicating a near-uniform abundance of all elements ($\sim \pm 0.1$ dex) relative to the Sun. The solid line shows a linear least-squares fit to these data, with the result that there is no measurable trend of abundance with T_c .

Fig. 9.— Slopes derived from [X/H] versus T_c for stars with planets from Gonzalez et al. (2001) and for HD19994. The average value of the slopes, with $\pm 1\sigma$ to this average, are shown by the vertical dashed lines. The error bars on the individual points are calculated from the goodness-of-fit to a straight line and individual errors in [X/H] of 0.1 dex. The two stars with the lowest (most negative) slopes are two of the most metal-poor stars in the sample. A small group of 5-6 stars falls at higher values for the slopes: these stars are possible candidates for fractionated accretion.

Fig. 10.— Derived slopes of [X/H] versus T_c are plotted as a function of [Fe/H] for three samples of stars (Edvardsson et al. 1993–BDP; Feltzing & Gustafsson 1998–FG; stars with planets from Gonzalez et al. 2001 and HD19994–SWP). There is a trend of decreasing T_c -slope with lower [Fe/H] caused by general chemical evolution in the disk (due mostly to the increase of [O/Fe] as [Fe/H] decreases). A small group of SWP points exist with larger T_c -slopes, as well as two FG high-metallicity stars. These stars are segregated from the general trend and are suggested to be the best candidates to have undergone possible fractionated accretion.

Fig. 11.— Abundances on the scale [X/H] versus elemental condensation temperature (T_c) for two stars from the six that were identified as having the largest trends of [X/H] versus T_c . In both of these stars, the abundances of the more volatile elements are ~ 0.3 dex lower than those from the more refractory species. This difference in abundance is significant and suggests selective mass accretion of refractory elements, possibly through the addition of solid material into their outer convective envelopes.

Fig. 12.— Orbital properties and masses ($M \sin(\iota)$) of the planets around stars exhibiting the largest slopes of [X/H] with T_c (filled circles), and those stars falling closer to the general trend of T_c -slope versus [Fe/H] (open circles). The top two panels show $M \sin(\iota)$ versus semi-major axis (a) and eccentricity (e), respectively. The most apparent trend in these two panels is that the stars with large T_c -slopes tend to have nearby companions. The bottom panel isolates e versus a and the stars with large T_c -slopes are clearly confined to the left part of the plot ($a \leq 1$ AU).

Fig. 13.— Cumulative fractional orbital separations, for all star–planet systems with measured abundances, are shown in the top panel. The cumulative fraction is the fraction of the sample that has an orbital separation, a , less than a particular value of a . In the bottom panel the sample

is split into those stars with the larger T_c -slopes, and the other systems which follow the general field disk trend of T_c -slope versus [Fe/H]. The distributions are markedly different: stars with large slopes (and are considered to be the best candidates to have undergone fractionated accretion) have companions that are significantly closer, on average, than stars showing no strong evidence of fractionated accretion.